TECHNION RESEARCH AND DEVELOPMENT FOUNDATION LTD.

OPTIMAL INTEGRATION OF ESTIMATION AND GUIDANCE FOR INTERCEPTORS

AFOSR Contract No. F61775-01-C-0007

Final Technical Report

covering the period of October 2001 – September 2004

Principal Investigators: Josef Shinar, Professor Emeritus
Yaakov Oshman, Associate Professor
Investigator: Vladimir Turetsky, Research Scientist

Faculty of Aerospace Engineering,
Technion, Israel Institute of Technology, Haifa, Israel.

Report Documentation Page

Form Approved
OMB No. 0704-0188

1. REPORT DATE	2. REPORT TYPE	3. DATES COVERED
02 JUN 2005	**N/A**	**-**

4. TITLE AND SUBTITLE	5a. CONTRACT NUMBER
Optimal Integration Estimation & Guidance for Interceptor Autopilot	5b. GRANT NUMBER
	5c. PROGRAM ELEMENT NUMBER
6. AUTHOR(S)	5d. PROJECT NUMBER
	5e. TASK NUMBER
	5f. WORK UNIT NUMBER
7. PERFORMING ORGANIZATION NAME(S) AND ADDRESS(ES) **Technion - Israel Institute of Science and Technology Technion City Haifa 32 000 Israel**	8. PERFORMING ORGANIZATION REPORT NUMBER
9. SPONSORING/MONITORING AGENCY NAME(S) AND ADDRESS(ES)	10. SPONSOR/MONITOR'S ACRONYM(S)
	11. SPONSOR/MONITOR'S REPORT NUMBER(S)

12. DISTRIBUTION/AVAILABILITY STATEMENT
Approved for public release, distribution unlimited

13. SUPPLEMENTARY NOTES
The original document contains color images.

14. ABSTRACT

15. SUBJECT TERMS

16. SECURITY CLASSIFICATION OF:			17. LIMITATION OF ABSTRACT	18. NUMBER OF PAGES	19a. NAME OF RESPONSIBLE PERSON
a. REPORT	b. ABSTRACT	c. THIS PAGE			
unclassified	**unclassified**	**unclassified**	**UU**	**106**	

Table of contents

List of figures

List of tables

Preface

The objective of this Final Technical Report of the multi-year AFOSR Contract No. F61775-01-WE018 is to outline the development of an innovative approach to *integrated estimation/guidance design* to be applied for the interception of maneuvering targets in the environment of noise-corrupted measurements. This Final Technical Report also presents a comprehensive summary of the multi-year investigation allowing to follow the steps of the algorithm development and to appreciate the substantial improvement in homing accuracy that has been achieved. Although the examples used in the simulations were motivated by lower tier endo-atmospheric Ballistic Missile Defense scenarios, the *integrated estimation/guidance design* is equally implementable for other interception tasks. In the simulation examples generic data were used and therefore the numerical results are only illustrative. Nevertheless, the results point out that the new *integrated estimation/guidance design* approach has the potential of achieving "hit-to-kill" homing accuracy even in extremely difficult interception scenarios.

Abstract

This report summarizes a multi-year investigation effort resulting in an innovative *integrated estimation/guidance design* algorithm for the interception of randomly maneuvering targets using noise-corrupted measurements. The algorithm is based on separating the tasks of model identification, state reconstruction and change detection, as well as assigning them to different estimators. The selection of the appropriate estimator for providing guidance information is accomplished by explicit logic-based use of the time-to-go. The homing guidance is performed by a differential game-based bounded control guidance law, modified for enhancing its efficiency in the terminal phase. The algorithm was derived using a planar linearized model, but it was implemented and validated in a generic nonlinear three-dimensional ballistic missile defense scenario. The simulation results demonstrate an exceptional homing performance improvement compared to earlier results and a potential to achieve “hit-to-kill” accuracy.

1. Introduction

The task of intercepting maneuvering targets has been a major challenge to the guided missile community. Until recently interceptor missiles were designed and used against aircraft type targets having a moderate maneuvering capacity. In such scenarios, the speed and the maneuverability of the missile largely exceeded those of the target. Due to the vulnerability of an aircraft structure, miss distances of the order of a few meters (compatible with the lethal radius of the missile warhead) were considered admissible. The threat imposed by tactical ballistic and cruise missiles attacking high value targets (probably with unconventional warheads), emphasized the challenge of intercepting anti-surface missiles by defensive guided missiles (ballistic missile defense and ship defense being example scenarios). These modern anti-surface missiles fly at very high speeds and their maneuvering potential in the atmosphere is comparable to that of the interceptors. Moreover, though they are not designed to maneuver, this potential can be made useful by a modest technical effort even by not sophisticated countries.

Successful interception of anti-surface missiles, carrying lethal warheads, much less vulnerable and more dangerous than an aircraft, requires a very small miss distance or even a direct hit (“*to hit a bullet with a bullet*”). Although non-maneuvering targets, emulating anti-surface missiles, were successfully intercepted recently [1-3], threats with high maneuver potential are anticipated in the future. Currently used guidance and estimation techniques will not be able to achieve the required homing accuracy against such targets. The reasons for this deficiency can be understood by reviewing the basics of missile guidance theory, as well as the 50 years history of guided missiles design practice.

Guidance theory points out that the main error sources responsible for non-zero miss distances are: (i) noisy measurements, (ii) non ideal dynamics of the guidance system, (iii) the contribution of target maneuvers, (iv) limited missile maneuverability leading to saturation. Nevertheless, simulation studies and flight tests have demonstrated that adequate maneuverability advantage of the interceptor can make the resulting miss distances sufficiently small.

All known missile guidance laws used at the present, including Proportional Navigation (PN), are based (assuming *perfect information*) on deterministic linearized constant velocity kinematical models using a linear quadratic optimal control concept (with unbounded control). Thus, the limited maneuver potential of the interceptor has not been explicitly taken into account. Although PN was derived on the basis of an intuitive kinematical concept [4], it was shown to be an optimal guidance law against non maneuvering targets, assuming ideal missile dynamics [5]. More advanced guidance laws have included the effects of non-ideal dynamics of the guidance system and the contribution of target maneuvers in the *generalized zero effort miss distance* and used a time-varying gain schedule [6]. For the contribution of the target maneuvers, their current value and future evolution must be known. Since it cannot be directly measured, the information on the current target maneuver has to be obtained by an observer. For the future evolution, for sake of simplicity, in most cases a constant target maneuver has been assumed.

Theory predicts that such a guidance law can reduce the miss distance to zero if (i) the assumption on the target behavior is correct, (ii) the measurements are ideally accurate and (iii) the lateral acceleration of the interceptor does not saturate.

Nevertheless, if the interceptor/target maneuver ratio is sufficiently high, the inevitable saturation occurs only very near the end of the interception and the resulting miss distance becomes negligibly small.

Interceptor guidance has to be performed in realistic interception scenarios, involving unknown random disturbances and noise corrupted measurements. As a consequence, estimators have become indispensable elements in every interceptor guidance system and the homing performance of the interceptor missile has been limited by the estimation accuracy. It has been of common belief in the guided missile community that estimators and guidance laws can be developed independently. This belief, leading to a comfortable design practice, has been based on assuming that both the *Certainty Equivalence Principle* and the associated *Separation Theorem* [7] hold. However, for realistic interceptor guidance with noise-corrupted measurements, bounded controls and saturated state variables, as well as non-Gaussian random disturbances, the validity of this assumption has never been proven. In most cases, such convenient design approach had been acceptable, because it succeeded to satisfy the performance requirements, due to the substantial maneuverability advantage of guided missiles over their manned aircraft targets. Applying the same suboptimal approach also for the interception of highly maneuvering targets results in unsatisfactory homing performance as reported in Refs. [8-10].

Since 1993 a research team at the Faculty of Aerospace Engineering at the Technion – Israel Institute of Technology in Haifa has been conducting investigations, sponsored by AFOSR, studying the problem of intercepting maneuvering targets. The first objective of the Technion research team has been to identify the origin of the

unsatisfactory performance in the interception of highly maneuvering targets. A thorough analysis of extensive simulation results was carried out in the framework of AFOSR Contract No. F61708-97-C-0004 (terminated in 2001). It was aimed at understanding how key parameters in the models of the interceptor missile and of the target affect the outcome of an engagement against highly maneuvering autonomous unmanned flying vehicles and found the main reasons responsible for the deficiency of currently used guidance and estimation techniques against such targets.

(a) The optimal control formulation requires knowledge of the future acceleration profile of the maneuvering target, which is never available. For this reason in the guidance laws constant target acceleration (or no acceleration) were assumed.

(b) The velocities in realistic interception scenarios are far from being constant. Lateral acceleration limits are not constant either, because in many scenarios, such as in ballistic missile defense, the altitude is also varying.

(c) The estimation process, necessary for an efficient guidance with measurement noise, introduces an inherent delay in the information on target maneuvers.

In order to alleviate the difficulties caused by these features an innovative design approach was developed and presented in several papers [11- 19]. It was based on three non-orthodox ideas:

(i) The interception scenario was formulated as a zero-sum pursuit-evasion game.

(ii) Time-varying velocity and maneuverability profiles were considered.

(iii) A guidance law taking into account the estimation delay was derived.

The application of these ideas yielded a substantial improvement in homing performance, as reported in recently published papers [20-22]. In spite of this improvement, a hit-to-kill accuracy could not be attained, because the estimation delay was only partially compensated and the variance of the residual (converged) estimation error could not be eliminated. For further improvement both the estimation delay and the variance of the residual estimation error have to be minimized, presenting contradictory requirements. Reducing the variance of the converged estimation error requires a narrow bandwidth, whereas short delays can be achieved only by using an estimator with a large bandwidth.

Based on these results, in October 2001 a new research program was initiated in the framework of AFOSR Contract No. F61775-01-C-0007. The goal of this research effort, planned for the three years, was "to develop a new estimation approach suitable for the requirements of accurate terminal guidance of interceptor missiles". The planned research consisted of several elements:

(i) An extensive critical review of the existing literature on estimation and guidance.

(ii) Selection of a set of relevant estimation approaches and testing them in generic interception scenarios, comparing their estimation errors and analyzing their associated homing performance.

(iii) Development of a new estimation/guidance approach based on the results of the investigation described in (ii).

(iv) An extensive Monte Carlo numerical study, assessing the performance of the new approach in a large variety of interception scenarios with different target maneuver models.

The objective of this Final Technical Report is to present a comprehensive summary of the results obtained and the lessons learned in this multi-year research study. The results obtained in the first two and half year of the contract were presented in detail in previous reports:

1) Interim Technical Report, October 2001 – March 2002 (ITR1);

2) Annual Technical Report , October 2002 – September 2002 (ATR1);

3) Interim Technical Report, September 2002 – March 2003 (ITR2);

4) Annual Technical Report, September 2002 – September 2003 (ATR2);

5) Interim Technical Report, September 2003 – May 2004 (ITR3);

as well as in several journal publications and conference papers [23- 32].

In this Final Technical Report the underlying theory and the main results are repeated for the sake of completeness, followed by the presentation of new results obtained during the last phase.

This report is organized as follows. In the next section, the interception problem of maneuvering anti-surface missile is formulated. This is followed by a brief review of deterministic optimal interceptor guidance concepts and their implementation in a scenario of noise-corrupted measurements. In section 4 the difficulties in finding a feasible optimal estimator for this task are discussed. In section 5 the main results of the previous Technical Reports are summarized, whereas the details are given in respective appendices. In section 6, recently obtained results, not covered by these earlier reports, are presented.

2. Problem Statement

2.1. Scenario description

Two scenarios of intercepting maneuvering anti-surface missiles seem to be of practical interest. The first one is a three-dimensional endo-atmospheric ballistic missile defense (BMD) scenario with time-varying parameters (velocities and acceleration limits). The second scenario is the interception of a low flying cruise missile that can be approximately described by a horizontal, constant speed model. For the sake of research efficiency (simplicity, repeatability and reduced computational load), the major part of the analysis and the simulations was performed using a planar constant speed model. The more complex generic BMD scenario was used mainly for validation or to investigate important three-dimensional effects.

In both scenarios, the homing endgame starts shortly before interception, as soon as the onboard seeker of the interceptor succeeds to “lock on” the target. The relative geometry is close to a head-on engagement. It is assumed that at this moment the initial heading error with respect to a collision course is small, and neither the interceptor nor the target is maneuvering. These assumptions facilitate linearization of the interception geometry, and decoupling of the original three-dimensional equations of motion to two identical sets in perpendicular planes.

2.2. Information structure

It is assumed that the interceptor measures range and range rate with good accuracy, allowing the computation of the time-to-go. However, the measurements of the line of sight angle are corrupted by a zero mean white Gaussian angular noise. The

interceptor's own acceleration is accurately measured, but the target acceleration has to be estimated based on the available measurements. The target has no information on the interceptor, but, being aware of an interception attempt, it can command evasive maneuvers at any time during the endgame and change the direction of the maneuver randomly.

2.3. Lethality model

The objective of the interception is the destruction of the target (the attacking anti-surface missile). In the reported investigation, the probability of destroying the target is determined by the following simplified lethality function.

$$P_d = \begin{cases} 1, & M \le R_k, \\ 0, & M > R_k, \end{cases} \tag{1}$$

where R_k is the lethal (kill) radius of the warhead and M is the miss distance. This model assumes an overall reliability of 100% of the entire guidance system.

2.4. Performance index

The natural (deterministic) cost function of the interception engagement is the miss distance. Due to the noisy measurements and the random target maneuvers, the miss distance is a random variable with an a priori unknown probability distribution function. A large number of Monte Carlo simulations can provide the cumulative probability distribution function of the miss distanses that allows comparing the homing performances of different guidance systems. Based on the lethality function (1), the efficiency of a guided missile depends on the lethal radius R_k of its warhead.

One of the possible figures of merit is the single shot kill probability (SSKP) for a given warhead, defined by

$$SSKP = E\{P_d(R_k)\} \quad (2)$$

where E is the mathematical expectation taken over the entire set of noise samples against any given feasible target maneuver. The objective of the guidance is to maximize this value. An alternative figure of merit is the smallest possible lethal radius R_k that guarantees a predetermined probability of success. In several recent studies the required probability of success has been assumed as 0.95, yielding the following performance index.

$$J = r_{95} = \arg\{SSKP = 0.95\} \quad (3)$$

2.5. Equations of motion

The analysis of a time-invariant interception endgame is based on the following set of simplifying assumptions:

(i) The engagement between the interceptor (*pursuer*) and the maneuvering target (*evader*) takes place in a (horizontal) plane.

(ii) Both the interceptor and the maneuvering target have constant speeds V_j and bounded lateral accelerations $|a_j| < (a_j)^{max}$ (j = E, P).

(iii) The maneuvering dynamics of both vehicles can be approximated by first order transfer functions with time constants τ_P and τ_E, respectively.

(iv) The relative interception trajectory can be linearized with respect to the initial line of sight.

In Fig. 1 a schematic view of the planar interception geometry is shown. The X axis of the coordinate system is in the direction of the initial line of sight.

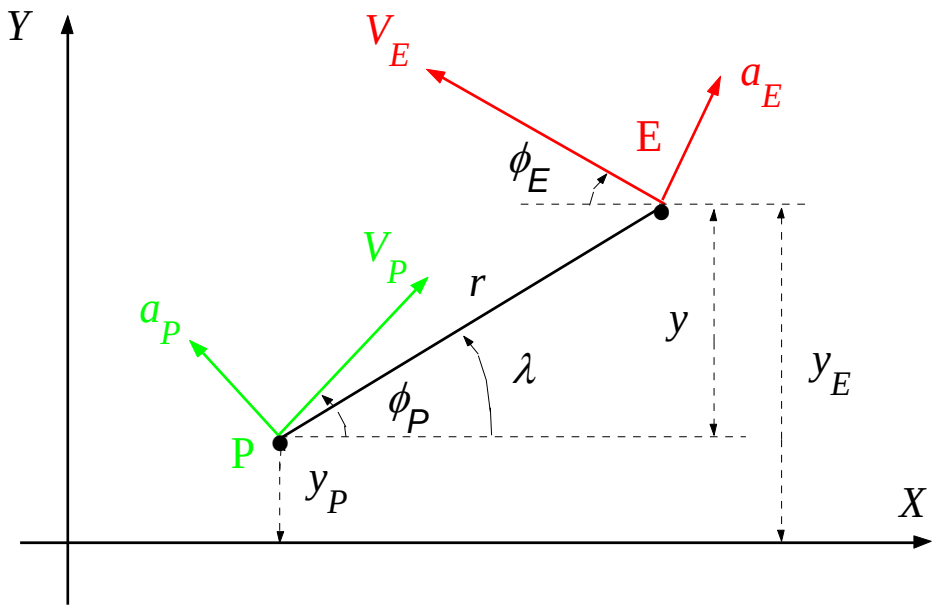

Fig. 1. Planar interception geometry

Note that the respective velocity vectors are generally not aligned with the reference direction. The aspect angles ϕ_P and ϕ_E are, however, small. Thus, the approximations $\cos(\phi_i) \approx 1$ and $\sin(\phi_i) \approx (\phi_i)$, (i = P, E), are uniformly valid and coherent with assumption (iv). Based on assumptions (ii) and (iv) the final time of the interception can be computed for any given initial range R_0 of the engagement by

$$t_f = R_0 / (V_p + V_E), \tag{4}$$

allowing to define the time-to-go by

$$t_{go} = t_f - t. \tag{5}$$

The state vector in the equations of relative motion normal to the reference line is

$$X^T = (x_1, x_2, x_3, x_4) = (y, dy/dt, a_E, a_P), \tag{6}$$

where

$$y(t) \stackrel{\Delta}{=} y_E(t) - y_P(t) \tag{7}$$

The corresponding equations of motion and the respective initial conditions are

$$\dot{x}_1 = x_2, \quad x_1(0) = 0, \tag{8}$$

$$\dot{x}_2 = x_3 - x_4, \quad x_2(0) = V_E \phi_{E_0} - V_P \phi_{P_0}, \tag{9}$$

$$\dot{x}_3 = (a_E^c - x_3)/\tau_E, \quad x_3(0) = 0, \tag{10}$$

$$\dot{x}_4 = (a_P^c - x_4)/\tau_P, \quad x_4(0) = 0, \tag{11}$$

where a_E^c and a_P^c are the commanded lateral accelerations of the target and the interceptor, respectively:

$$a_E^c = a_E^{max}\ \mathbf{v};\ |\mathbf{v}| \le 1, \tag{12}$$

$$a_P^c = a_P^{max}\ \mathbf{u};\ |\mathbf{u}| \le 1, \tag{13}$$

The nonzero initial conditions $V_E \phi_{E_0}$ and $V_P \phi_{p0}$ represent the respective initial velocity components not aligned with the initial (reference) line of sight. By assumption (iv) these components are small compared to the components along the

line of sight. The set of equations (8)-(11) can be written in a compact form as a linear, time invariant, vector differential equation

$$d\mathit{X}/dt = A\mathit{X} + Bu + Cv. \tag{14}$$

The problem involves two non-dimensional parameters of physical significance: the pursuer/evader maximum maneuverability ratio

$$\mu \stackrel{\Delta}{=} (a_P)^{max} / (a_E)^{max}. \tag{15}$$

and the ratio of the evader/pursuer time constants

$$\varepsilon \stackrel{\Delta}{=} \tau_E/\tau_P \tag{16}$$

The miss distance (the deterministic cost function), can be written as

$$M = |DX(t_f)| = |x_1(t_f)|, \tag{17}$$

where

$$D = (1, 0, 0, 0). \tag{18}$$

2.6. Game formulation

There is a basic deficiency in formulating the interception of a maneuverable target as an *optimal control* problem. Target maneuvers are independently controlled. Since future target maneuver time history (or strategy) cannot be predicted, the *optimal control* formulation is not appropriate. The scenario of intercepting a maneuverable target has to be formulated as a *zero-sum differential game of pursuit-*

evasion. In such a formulation, there are two independent controllers and the cost function is minimized by one of them and maximized by the other.

Based on the above outlined assumptions and formulation, several deterministic zero-sum pursuit-evasion game models were solved. The game solutions provided simultaneously the interceptor's guidance law (the *optimal pursuer strategy*), the "worst" target maneuver (the *optimal evader strategy*) and the resulting guaranteed miss distance (the saddle-point *value* of the game). In the next section the optimal guidance laws based on these game solutions are briefly described.

3. Game Optimal Guidance Laws

3.1. DGL/1

The first model that was solved (more then two decades ago) was a *perfect information* game [34], assuming that all the state variables and the game parameters are known to both *players.* The set of assumptions (i) – (iv) allowed casting the problem to the canonical form of linear games, from which a reduced order game with only a single state variable, the *zero effort miss distance* denoted Z, was obtained. As the independent variable of the problem, the time-to-go (t_{go}), defined by (5), was selected. The solution of this game is determined by the two parameters of physical significance μ and ε, defined by (15) and (16). The solution results in the decomposition of the reduced game space (t_{go}, Z) into two regions of different strategies, as can be seen in Fig. 2.

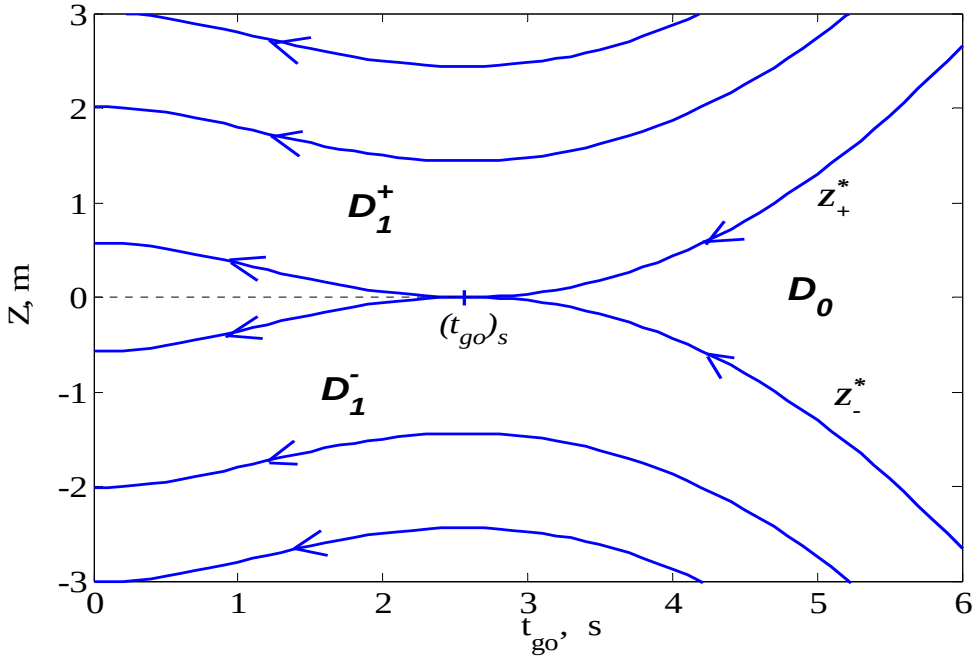

Fig. 2. Decomposition of the reduced game space

These regions are separated by the pair of optimal boundary trajectories denoted respectively by Z^*_+ and Z^*_-, reaching tangentially the Z = 0 axis at $(t_{go})_s$, where $(t_{go})_s$ is the non zero root of the equation $dZ/dt_{go} = 0$. One of the regions is a regular one, denoted by $\boldsymbol{D}_1$, where the optimal strategies of the players are of the "bang-bang" type

$$u^* = v^* = \text{sign}\{Z\} \quad \forall \quad Z \neq 0 \tag{19}$$

u and **v** being the normalized controls of the *pursuer* (interceptor) and the *evader* (the maneuvering target) respectively. The explicit expression for *Z* is

$$Z = x_1 + x_2\, t_{go} - \Delta Z_P + \Delta Z_E. \tag{20}$$

where

$$\Delta Z_P = x_3 (\tau_P)^2 [\exp(-\theta_P) + \theta_P - 1] \quad (21)$$

$$\Delta Z_E = x_4 (\tau_E)^2 [\exp(-\theta_E) + \theta_E - 1] \quad (22)$$

while $\theta_P = t_{go}/\tau_P$ and $\theta_E = t_{go}/\tau_E$.

The value of the game in this region is a unique function of the initial conditions. The boundary trajectories themselves also belong to $\boldsymbol{D}_1$. Inside the other region, denoted by $\boldsymbol{D}_0$, the optimal strategies are arbitrary and the value of the game is constant, depending on the parameters of the game (μ, ε). If the parameters of the game are such that $\mu\varepsilon \geq 1$, then the only root of the equation $dZ/dt_{go} = 0$ is zero and the value of the game in $\boldsymbol{D}_0$ is also zero. (Note that the "bang-bang" strategies (19) are also optimal in $\boldsymbol{D}_0$). The practical interpretation of the game solution is the following:

(i) the optimal missile guidance law can be selected as (19) during the entire endgame;

(ii) the worst target maneuver is a constant lateral acceleration starting not later than $(t_{go})_s$;

(iii) the guaranteed miss distance depends on the parameters (μ,ε) and can be made zero if $\mu\varepsilon \geq 1$.

In this case, $\boldsymbol{D}_0$, which includes all initial conditions of practical importance, becomes the "capture zone" of this *perfect information* game. Implementation of the optimal missile guidance law, denoted as DGL/1, requires the perfect knowledge of the zero effort miss distance, which includes also the current lateral acceleration of the target.

3.2. DGL/E

The second model is also a planar *perfect information* game, but with time varying velocities and maneuverabilities. The maneuver plane in this model is the vertical plane, allowing variations also in altitude (and consequently in air density). In this game, assumption (ii) is replaced by assuming that profiles of these variables are known along a nominal trajectory.

Such a model is the suitable one for the analysis of a realistic BMD endgame scenario. The solution of this game [11, 20], is qualitatively similar to the previous one (DGL/1), but depends strongly on the respective velocity/maneuverability profiles of the *players* and obviously, the value of μ is not constant. Due to the time varying profiles, the expressions of the *zero effort miss distance*, as well as of $(t_{go})_s$ and the guaranteed miss distance, become more complex.

In spite of this (algebraic) complexity, the implementation of the optimal missile guidance law, denoted as DGL/E, doesn't present essential difficulties. It requires, of course (in addition of the perfect knowledge of the current lateral acceleration of the target), the velocity and maneuverability profiles in the endgame that can be precalculated along a nominal trajectory.

3.3. DGL/C

As mentioned earlier, the implementation of the *perfect information* guidance laws DGL/1 and DGL/E require the knowledge of the target lateral acceleration. Since this variable cannot be directly measured, it has to be estimated based on noise corrupted measurements. If the *pursuer* uses DGL/1, derived from the perfect information game solution [33] the *evader* can take advantage of the estimation delay and achieve a large miss distance by adequate optimal maneuvering [34], as seen in by the red curve in Fig. 3, even if the game parameters are such that the guaranteed miss distance should be zero.

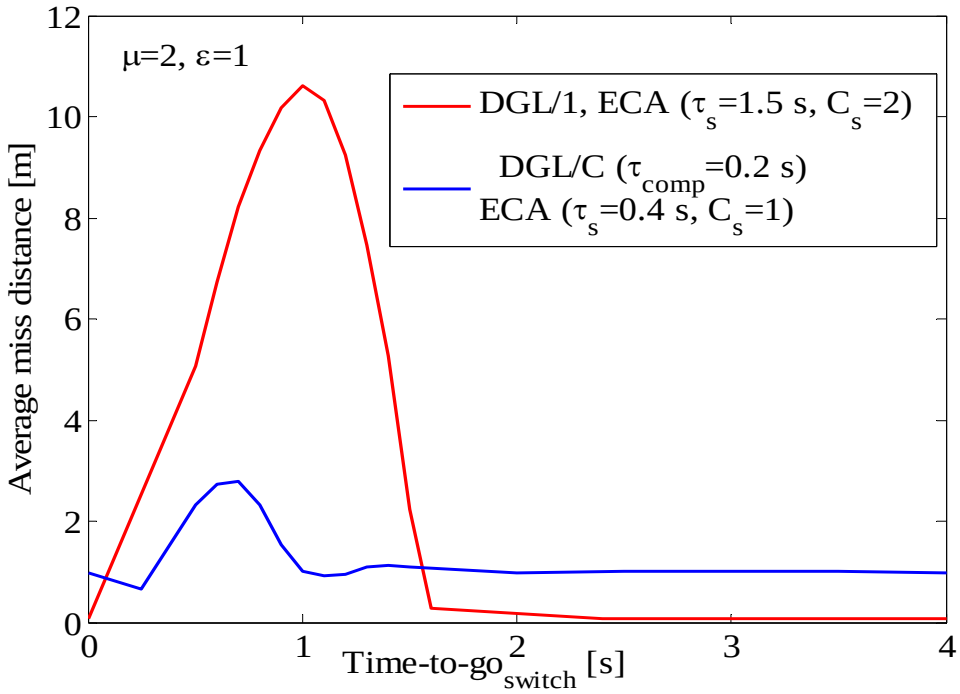

Fig. 3. Homing performance of DGL/1 and DGL/C against "bang-bang" target maneuvers

Fig. 3 represents the average miss distance of 100 Monte Carlo simulation runs as a function of the direction reversal timing (switch) in the target maneuver. The data used for these simulations are given in Table 1.

Table 1. Horizontal end game parameters

Parameter	Value
Interceptor velocity	V_P = 2300 m/sec
Target velocity	V_E = 2700 m/sec
Interceptor lateral acceleration limit	a_P^{max} = 20 g
Target lateral acceleration limit	a_E^{max} = 10 g
Time constant of the interceptor	τ_P = 0.2 sec
Time constant of the target	τ_E = 0.2 sec
Initial end game range	R_0 = 20 km
Duration of end game engagement	t_f = 4 sec
Measurement noise	σ_{ang} = 0.1 mrad

In the simulations a typical Kalman filter [35], augmented with a shaping filter, was used. Such a shaping filter, driven by a zero mean white noise represents random target maneuvers [36]. The shaping filter selected for this case was based on an exponentially correlated acceleration (ECA) model, suggested by Singer [37]. Such a shaping filter has first order dynamics with two tuning parameters, the correlation time of the maneuver τ_s and the level of the assumed process noise, expressed by its standard deviation $\sigma_s = a_E^{max}/C_s$. In this example the parameters of the shaping filter were τ_s = 1.5 s and C_s = 2.

The main reason for the degraded homing performance is the inherent delay introduced by the convergence time of the estimation process. Based on this observation, a rough approximation of the estimation process assumed that the evader's lateral acceleration is a *delayed* (perfect) outcome by τ_{est}, while the

estimation of the other state variables is ideal. This modeling assumption allowed a deterministic analysis and a new *pursuit-evasion game* was formulated and solved. The solution of this planar *"delayed information"* game [14 -16], assuming for the sake of simplicity constant velocities and lateral acceleration bounds, was based on the idea of *reachable sets* [38] suggested for such problems. In order to compensate for the estimation delay ($\tau_{comp} = \tau_{est}$), this approach suggested that the *zero effort miss distance* Z is replaced by the center of the *uncertainty set* created by the estimation delay, denoted as Z_c. The explicit expression of Z_c is

$$Z_c = x_1 + x_2 t_{go} - \Delta Z_P + (\Delta Z_E)_c, \tag{23}$$

where

$$(\Delta Z_E)_c = \Delta Z_E \exp(-\tau_{est}/\tau_E). \tag{24}$$

The decomposition of the reduced game space (t_{go}, Z_c) seems qualitatively similar to Fig. 2. The solution yielded a guidance law, denoted as DGL/C, which compensates (at least partially) for the inherent estimation delay [14-16]. A deterministic analysis [14] showed that using this guidance law a substantial reduction of the guaranteed miss distance can be achieved, but the guaranteed miss distance cannot be reduced to zero. It is a monotonically increasing function of the estimation delay divided by the time constant of the *evader* ($\delta = \tau_{est}/\tau_E$).

Testing this guidance law in a noise corrupted endgame scenario [17], using an estimator with the shaping filter parameters $\tau_s = 0.4$ s, $C_s = 1$ and the time delay to be compensated set to $\tau_{comp} = \tau_{est} = 0.2$ sec, indeed confirmed a substantial reduction of the "worst case" miss distance compared to DGL/1, on the expense of increased miss distances in the range of $1.6 \text{ sec} < (t_{go})_{sw} < 4.0$ s (where DGL/1 yielded excellent

precision), as shown in Fig. 3 by the green curve. Moreover, if the timing of the eventual change in the direction of the target maneuver is assumed to be uniformly distributed, the reduction in the average miss distance is not as impressive.

The practical difficulty in implementing DGL/C is to determine the value of τ_{est} to be used in the expression of Z_c. This value depends on both the structure and the parameters of the estimator, as well as on the measurement noise model. For a given estimator and noise, the value of τ_{est} that optimizes the miss distance distribution against the "worst" target maneuver has to be found by a min-max search using off-line Monte Carlo simulations.

3.4. DGL/EC

The two different improvement features, developed using planar linearized interception models (DGL/E with *perfect information* and time varying velocities, DGL/C with constant velocities and *delayed* information), were integrated into a single (planar) guidance law denoted as DGL/EC [22]. This planar guidance law was implemented in two perpendicular guidance channels of a roll-stabilized interceptor missile and tested in simulations of a generic but realistic noise corrupted nonlinear ballistic missile defense scenario by using a suitable three-dimensional estimator.

The simulation results confirmed an additional homing performance improvement compared to either DGL/E or DGL/C. However, the guaranteed homing accuracy was not sufficient for a "hit to kill" for two reasons. The estimation delay was only partially compensated and the residual estimation error was neglected in the deterministic analysis. For an improved homing performance, both the estimation

delay and the variance of the converged estimation error have to be reduced. Therefore, further investigations, using extensive simulations, had to be aimed to search an improved estimation scheme suitable to the interception endgame problems, which became the goal of the AFOSR Contract No. F61775-01-C-0007. The next section outlines the problems involved in reaching this goal.

4. Estimation

4.1. Estimators and shaping filters

As indicated in subsection 2.2, it is assumed that the interceptor measures range and range rate with good accuracy, allowing a computation of the time-to-go. However, the measurements of the line of sight angle, carried out at the frequency of 100 Hertz, are corrupted by a zero mean white Gaussian angular noise with a given variance. The interceptor's own acceleration is accurately measured, but the target acceleration has to be estimated, based on the available measurements.

In the framework of AFOSR Contract No. F61775-01-C-0007 several different types of discrete time estimators were tested. The family of estimators was based on the well known "classical" Kalman filter (KF) [35] with a zero mean white noise driven shaping filter (SF) representing the random target maneuvers [36]. Several types of shaping filters corresponding to different target maneuver models were used.

One of the models assumes maximum maneuver with random starting time (RST). The RST/SF is an integrator driven by zero mean white noise. The spectral

density of the noise is proportional to the square of the maximum target lateral acceleration and inversely proportional to the duration of the endgame: $\sigma_r^2 = \frac{\left(C_r a_{E_{max}}\right)^2}{t_f}$, where C_r is a tuning parameter. This estimator turns out to be unbiased and its delays in estimating the relative lateral velocity and the lateral target acceleration are proportional to the value of the tuning parameter C_r.

The other model is the exponentially correlated acceleration (ECA) model of Singer [37]. The ECA/SF has first order dynamics with a time constant τ_s, inversely proportional to the assumed average frequency of target maneuver switches. The value of τ_s serves as a second tuning parameter (in addition to the factor C_s defined by $\sigma_s = a_E^{max}/C_s$). It turns out that in this filter (particularly when used to estimate "bang-bang" type maneuvers) the estimation delay is proportional to the value of τ_s. Moreover, the filter provides biased estimates of the relative lateral velocity and the lateral target acceleration. For both variables, the magnitude of the estimated variables is smaller than the actual ones. The biases are inversely is proportional to the value of τ_s.

Since one type of the tested random maneuvers is sinusoidal, a periodical shaping filter (PSF) of second order dynamics [36], tuned to an assumed frequency ω_f , was also used in some of the simulations. In this filter the spectral density of the noise is proportional to the square of the maximum target lateral acceleration and the proportionally factor ($1/C_p$) serves as a second tuning parameter.

4.2. On optimal estimation

In the search of a suitable optimal estimator for the task of intercepting randomly maneuvering targets, several difficulties have been encountered. The basic one has been of a conceptual nature. For linear systems with zero-mean, white and Gaussian measurement and process noises, the Kalman filter [35], based on the correct model of the system dynamics, is known to be the optimal estimator in the sense of minimum variance of estimation error. The measurement noise used in interception simulations has indeed such characteristics, but the representation of a random target maneuvers as the output of a "shaping filter" driven by a zero-mean, white, Gaussian noise [36] is only an approximation. Moreover, each type of target maneuver requires a different "shaping filter" approximation. Since target maneuver dynamics is not ideal, the target acceleration is a state variable, a part of the interception model. The disturbance inputs are the random acceleration commands and can be discontinuous, representing a random jump process. They are bounded and certainly neither white nor Gaussian.

In several recent papers [39-40], it was shown that in such cases the *optimal estimator* is of infinite dimension. Thus, every computationally feasible (finite dimensional) estimator can be, at best, only a suboptimal approximation and the search for a feasible *optimal estimator* associated with interceptor guidance is not a well-posed problem. Similarly, it should be of no surprise that the *Certainty Equivalence Principle* and the associated *Separation Theorem*, both involving the concept of *optimality*, are not valid for the interception of randomly maneuvering targets. Not being able to rely on separate optimization of the estimator and the guidance law, one should search for efficient feasible approaches.

In cases where the *Certainty Equivalence Principle* cannot be proven, a "partial" *separation* property was asserted [41], stating that the estimator can be designed independently of the controller, but the derivation of the optimal control function has to be based on the conditional probability density function (conditioned on the measurement history) of the estimated state variables. Unfortunately, a rigorous practical approach implementing this idea has not yet been developed and applied in any known control design including guided missiles. An attempt in this direction was made in the development of the guidance law DGL/C [14-16], partially compensating the estimation delay, but this was only an approximation that neglected the stochastic features of the problem caused by the effects of the noisy measurements, namely the variance of the residual (converged) estimation error.

The requirements to reduce both the estimation delay and the variance of the converged estimation error, mentioned earlier, are contradictory. The convergence time associated with identifying a rapid target maneuver change is composed of the maneuver detection time and the estimator's response time. Short detection time comes at the price of high false alarm rate, while short response time requires large bandwidth, generating large estimation errors. Good filtering, providing a small estimation error variance, requires narrow bandwidth leading to a slow response.

This controversy has raised the question: *Can a single estimator satisfy the contradictory requirements of homing accuracy?* In the absence of available theory, the answer was sought in extensive Monte Carlo simulations [42]. Theses simulation studies lead to conclude, as was summarized in the reports of the first year (ITR1 and ATR1), that no estimator is globally optimal for all guidance laws/interception

scenarios and there is no unique "optimal" estimator/guidance law combination for all feasible target maneuvers. The answer on the above raised question being negative, a new approach had to be developed. This approach has been based on an *integrated estimation/guidance design* [43] pursued in the consecutive phases of the research program involving multiple model estimators [44-45]. In the next section the results obtained during the three years of the investigation effort, as presented in the different Technical Reports, are summarized.

5. Previous Results

The first year of investigations in the framework of AFOSR Contract No. F61775-01-C-0007 was devoted to exploring and understanding how different combinations of estimators and guidance laws affect the *guaranteed* homing performance. In this phase on an extensive parametric study, using a planar constant speed model was performed. Based on the results obtained in the first year, the research effort in the second and third years was oriented to develop a suitable *integrated estimation/guidance design* that has the potential of achieving hit-to-kill homing accuracy. In addition to planar constant speed simulations, a generic three-dimensional BMD scenario was also used.

5.1. First year (October 2001-September 2002)

5.1.1. ITR1. (October 2001-March 2002)

The very large number (more than 100,000) of Monte Carlo simulations performed during this period concentrated on the "worst" case homing performance against the "worst" feasible target maneuver. Based on the results of the perfect

information game solutions and earlier simulation studies, the target maneuver was assumed to be of the “bang-bang” type with random timing and the “worst” timing of the maneuver command change was identified. The homing performance was characterized by the cumulative miss distance distribution, based on 100 Monte Carlo simulation runs, against this “worst” target maneuver. The main results of these simulations, expressed by the values of r_{95} (indicating the largest miss distance of 95% of the samples) were the following:

1, The simulation results provided an experimental demonstration that for the interception of a randomly maneuvering target the *Certainty Equivalence* property and the associated *Separation Theorem* are not valid. The guidance law derived from the perfect information game solution (DGL/1) is not optimal in a noise corrupted measurements scenario, where an estimator is incorporated in the guidance loop. Other guidance laws, such as DGL/C and in some cases even DGL/0 [46–47] (a guidance law that assumes ideal target dynamics, i.e. $\tau_E = 0$,), have better homing performance.

2, The homing performance of the delay compensating DGL/C is superior (as could be expected) to the other guidance laws, but a “hit-to-kill” accuracy against a 10g target maneuver (with 20g own lateral acceleration limit and angular measurement noise level of σ_a=0.1 mrad) cannot be achieved.

3, The derivation of DGL/C, associated with finding τ_{comp} the delay compensation term of the guidance law, turned out to be rather complex. For a given set of estimator tuning parameters, the best value of τ_{comp} can be found. However, the very value of τ_{comp} affects the selection of the best tuning parameters for a given estimator structure. Finding the best combination has required a simultaneous min-max search in the joint estimator/guidance law parameter space.

4, The ensemble average of the estimation error in the “worst” case was also evaluated. From the ensemble average of the estimator output data one can observe that there is a delay not only in the estimated lateral target acceleration, but also in the estimated relative lateral velocity. Moreover, the estimation delay of this state variable is not the same as the estimation delay of the lateral target acceleration and neither of these delays remains constant during the endgame.

5, The relationship between the actual estimation delay in detecting a change in lateral target acceleration (as it is measured from the ensemble average of the estimator data) and the best value of τ_{comp} used in the DGL/C guidance law is not clear. The best value of τ_{comp} doesn’t have either a direct relationship with the predicted value of the minimum time needed to detect target maneuver change [48-49].

6, It is also observed that using DGL/C the difference between the homing performances of the various estimators is much smaller than with the other guidance laws, because DGL/C corrects, at least partially, the deficiencies of the estimators.

7, The cumulative distribution of the “worst” case miss distances (for a given estimator and guidance law combination) can be approximated as the sum of two parts: a “deterministic” minimal miss distance, due to the partially compensated estimation delay, and a random part with a Rayleigh type probability distribution. Such distribution is characterized by a single parameter, which can be associated with the variance of the residual (converged) estimation error. Both values are monotonic functions of the measurement noise variance, depending on the estimator model and its parameters.

The detailed results of ITR1 are presented in Appendix A.

5.1.2. ATR1. (April - September 2002)

In this period of March 2002 to September 2002 a new set of Monte Carlo simulations was performed, intending to test and compare the homing performance of several estimator/guidance law combinations with two measurement noise levels (σ_a = 0.1/0.2 mrad) and different maneuverability ratios ($1.5 \leq \mu \leq 3.0$) against two types of random target maneuvers:

(i) a “bang-bang” maneuver randomly switched during the interception endgame;

(ii) a sinusoidal maneuver with random phase, representing the planar projection of a three-dimensional “spiral” maneuver [50].

Based on these simulation results and those of ITR1, all assuming planar constant speed scenarios, a set of new conclusions were reached.

1, The simulations confirmed that against a randomly switching “bang-bang” type maneuver, DGL/C is the best of the known guidance law. However, the homing performance using this guidance law strongly depends on the type and the parameters of the estimator incorporated in the guidance loop.

2, The two-dimensional simulations against sinusoidal maneuvers with random phase, representing the planar projection of a three-dimensional “spiral” maneuver [50], showed that such maneuvers are less demanding, from the interceptor’s point of view, than “bang-bang” type maneuvers. The reasons are the lower maneuver energy compared to a “bang-bang” maneuver of the same maximal

amplitude and the gradual change in the acceleration command. (In the three-dimensional case, investigated in the framework of AFOSR Contract No. F61775-01-WE018, the maneuvering energies of the two maneuver types were the same. Thus, in a three-dimensional interception scenario some “spiral” maneuver created larger miss distances than a “bang-bang” type when for both the same estimator/guidance law combination, -the best against the worst case “bang-bang” maneuver,- was used.)

3, It was also demonstrated that against sinusoidal maneuvers a much better homing performance can be achieved if the estimator uses a matched periodical shaping filter (PSF) instead of the one used against the “bang-bang” maneuver. Moreover, against sinusoidal maneuvers the guidance law DGL/1 has better homing performance than DGL/C.

4, The sensitivity of the homing performance against sinusoidal maneuvers to the mismatch between the maneuver frequency and the periodical shaping filter can be reduced at the expense of slightly worse minimum average miss distance. If the maneuvering frequency is completely unknown, an estimator with ECA shaping filter can serve as a compromise.

5, Based on the above findings, it seems necessary to use some kind of multiple model estimator [44-45], which can identify the maneuver type and select the best one from a family of assumed estimators.

The detailed results of ATR1 are presented in Appendix B.

5.2.Second year, (October 2002-September 2003)

5.2.1. ITR2. (October 2002-March 2003)

Based on the conclusions obtained from earlier results in this year the research effort was focused on developing a suitable integrated estimation/guidance design that leads to an improved accuracy. Since no estimator is globally optimal for all guidance law/interception scenarios and there is no unique “optimal” estimator/guidance law combination for all feasible target maneuvers, the initial phase of the endgame has to be devoted to identifying the type of target maneuver using a multiple model estimator [44]. It was assumed that the target can perform one of the following maneuver options:

(i) no maneuver,

(ii) a continuous sinusoidal maneuver of a given frequency with a random phase,

(iii) a constant maximum lateral maneuver with a random initiation time,

(iv) a maximum lateral maneuver to one side, switching at a random time to the opposite side.

It was found that, for this purpose, a classical, static (non interactive), multiple model adaptive estimation (MMAE) approach is suitable. As long as the target maneuver has not been identified, the objective of the guidance law should be to correct the initial errors. During that initial phase, since the target maneuver is uncertain, a guidance law that does not require the knowledge of target maneuver, such as DGL/0, was used. Once the target maneuver model has been identified, the guidance has to be switched to DGL/1 with the best available estimator corresponding to the identified maneuver model.

In the case where a constant (including zero) maneuver is identified, DGL/1 with a narrow bandwidth estimator (that minimizes the variance of the converged estimation error) can guarantee small miss distances, if either the maneuver remains constant, or an eventual direction switch takes place early enough (before a critical time-to-go is reached), as shown in Fig. 3 in subsection 3.3. In such cases, the effect of the inherent estimation delay becomes negligible**.** If a target maneuver command "jump" has been identified before the critical time-to-go (1.6 sec in the example shown in Fig. 3), the probability for an additional jump to occur before the end becomes very low, because the target designer has no interest in too frequent maneuver changes that cannot create large miss distances. Thus, in this case using DGL/1 should continue.

If until the critical time-to-go no maneuver command "jump" has been identified, the guidance law was switched to DGL/C in order to avoid large miss distances that are created by DGL/1 if a "jump" in the target maneuver command occurs later. The homing performance of this guidance law can be improved if the estimator is *tuned* to assume a step change in the maneuver command at a preselected time-to-go. A few (3 in the simulation example) preselected *tuned* estimators covered the range of interest. Implementation of this idea required an innovative use of the time-to-go in the estimator selection, not known to be used in other works.

In the case of sinusoidal target maneuvers it was observed that if the maneuver frequency used in the PSF estimator is correct, excellent homing performance can be obtained using DGL/1 as a guidance law. Moreover, if the estimation error (depending on the frequency mismatch of the estimator’s shaping filter) is not too

large, the homing performance is still acceptable. If the process noise level used in the PSF estimators is not too low a few shaping filters of different frequencies cover reasonably well the domain of expected maneuver frequencies.

The simulation results, carried on separately for "bang-bang" type maneuvers assuming uniformly distributed random "jump" and for sinusoidal maneuvers with uniformly distributed random phase, were very encouraging. The performance improvement achieved by the use of the time-to-go information against randomly switched "bang-bang" target maneuvers is outstanding. The new approach preserves the excellent performance of DGL/1 until the critical time-to-go (in about 60% of the runs). In addition, by using the *tuned* estimators associated with DGL/C, the method provides improved performance as compared to earlier results with a non-tuned estimator, as can be seen in Fig.4.

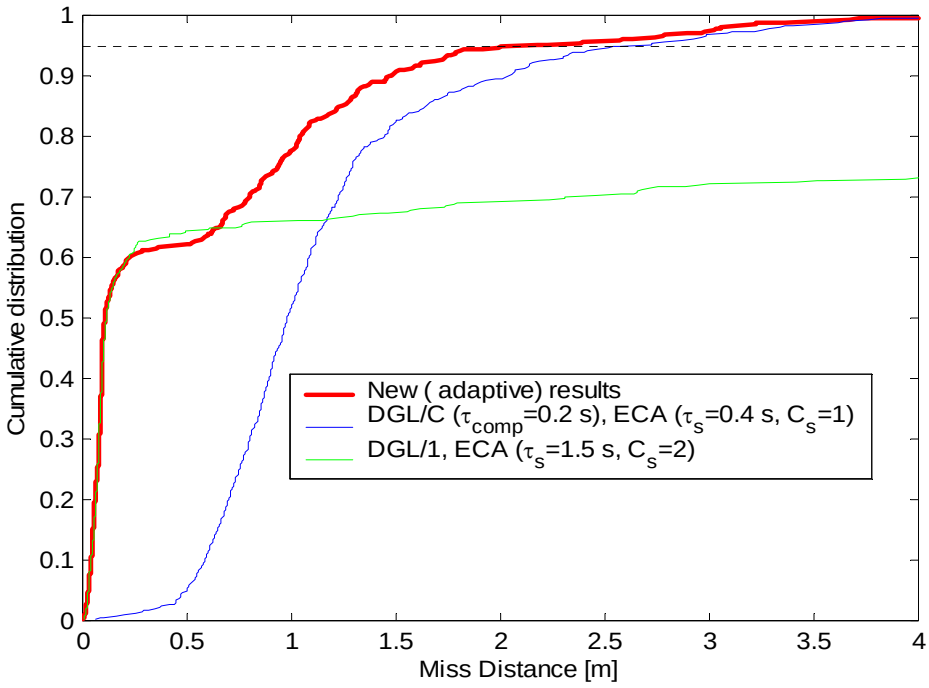

Fig. 4. Cumulative miss distance probability distribution against randomly switching "bang-bang" target maneuvers

The new approach preserves the excellent performance of DGL/1 until the critical time-to-go (in about 60% of the runs). In addition, by using the *tuned* estimators associated with DGL/C, the method provides improved performance as compared to earlier results with a non-tuned estimator. The improvement is also expressed by the average miss distances of the 500 Monte Carlo runs, being 0.57 m for the new approach, compared to1.16 m for DGL/C and 2.40 m for DGL/1.

The results against sinusoidal random phase maneuvers were even better, as can be seen in Fig. 5. The required kill radius for 0.95 kill probability against such maneuvers is only about 0.5 m, as compared to a much higher value (about 2 m) against bang-bang maneuvers, and the average miss distance is only 0.19 m.

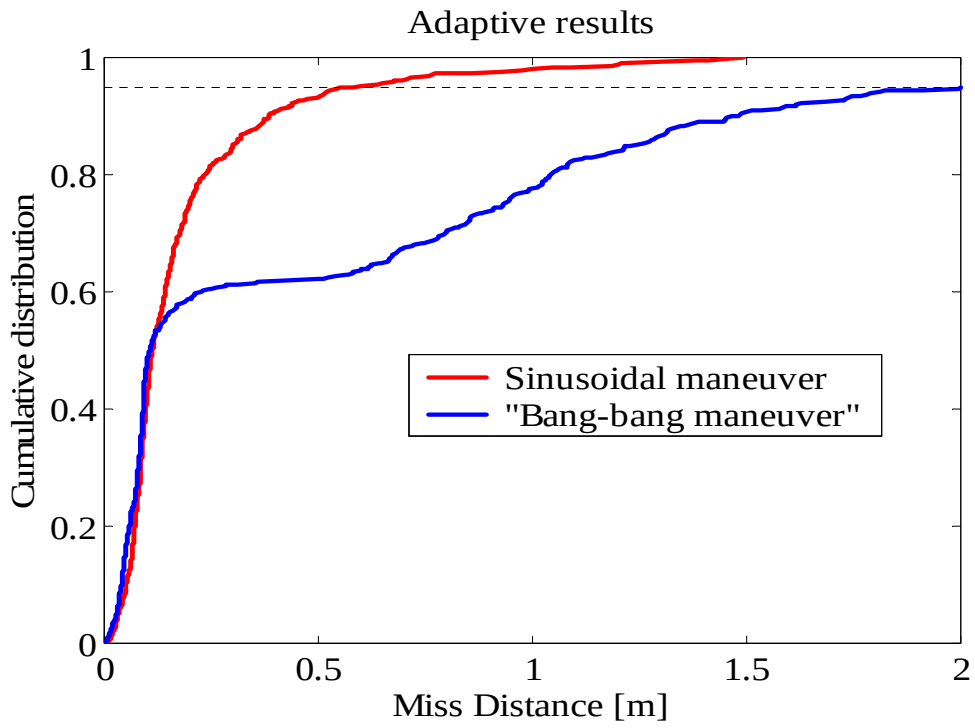

Fig. 5. Cumulative miss distance probability distribution against random target maneuvers.

The estimator equations used in the simulations are presented in Appendix C.

5.2.2. ATR2. (April - September 2003)

The results presented in ITR2 showed excellent performance against random phase periodical maneuvers in a wide frequency range. The homing performance against “bang-bang” type maneuvers with a random switch was also improved, compared to earlier results, but a potential of further improvement was also observed. In the second part of the contract's second year the investigation effort was oriented to exploit this improvement potential. The improvement potential of the interceptor homing performance is explored by a different implementation of the multiple model adaptive estimation/guidance concept, based on explicit use of the time-to-go and the properties of a “tuned” estimator. The first phase in this direction was to evaluate the homing performance of DGL/1 with several “tuned” estimators for different timings of the switch in the target acceleration command. The estimators for this evaluation used ECA shaping filters with a relatively large bandwidth (τ_s = 0.2 sec and C_s = 3).

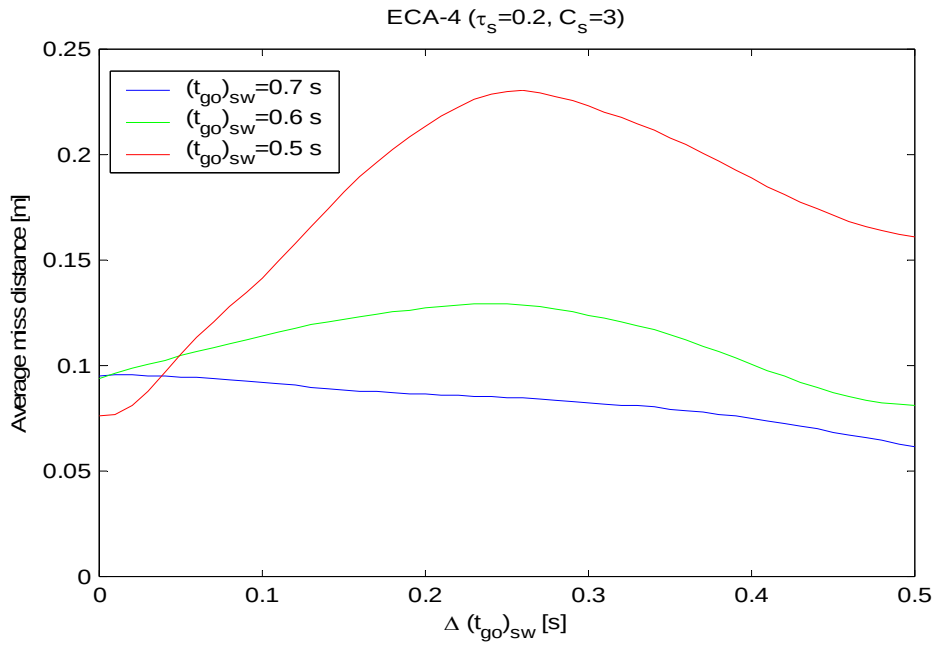

Fig. 6. Homing performance with “tuned” estimators

The results presented in Fig. 6 show the average miss distances of 100 Monte Carlo runs for three different values of $(t_{go})_{sw}$, (the time instant of the target maneuver command change in the sensitive zone near the end) as a function of $\Delta(t_{go})_{sw}$, (the difference between the "tuning time" of the estimator and the true value of $(t_{go})_{sw}$). Positive values of $\Delta(t_{go})_{sw}$ indicate that the estimator is tuned for an earlier switch (larger time-to-go). This figure shows miss distances of the order of a few cm and a surprisingly excellent robustness, allowing to use only very few "tuned" estimators.

These results indicated that if the identified target maneuver in the initial phase is constant, then in the new estimation/ guidance strategy DGL/1 has to be preferred over DGL/C. Assuming that the event of the "jump" in the target acceleration command can be detected sufficiently fast, the robustness property displayed in Fig 6 suggested that after the critical time-to-go (as soon as the jump in the direction of the target maneuver command is detected) the narrow bandwidth estimator, providing the input of DGL/1, be replaced by the nearest (earlier) "tuned" wide bandwidth version. Three "tuned" estimators (t_{sw} = 1.5, 1.0, 0.5 sec) covered the range of interest.

This new estimation/guidance concept was tested by extensive Monte Carlo simulations for every 0.1 sec of $(t_{go})_{sw}$ within the 4 sec duration of the benchmark endgame, using 100 noise samples for each. The results, based on the assumption of *ideal* detection, are indeed excellent. Fig. 7 displays the cumulative miss distance probability distribution, which is very close to satisfying the hit-to-kill requirement.

Since an *ideal* detection of the jump in the direction of the target maneuver command is not feasible, the Monte Carlo simulations were repeated assuming small detection delays of 0.05 and 0.1 sec. The cumulative miss distance probability distributions for these two cases together with the earlier results (of Fig.4) are also shown in Fig.7.

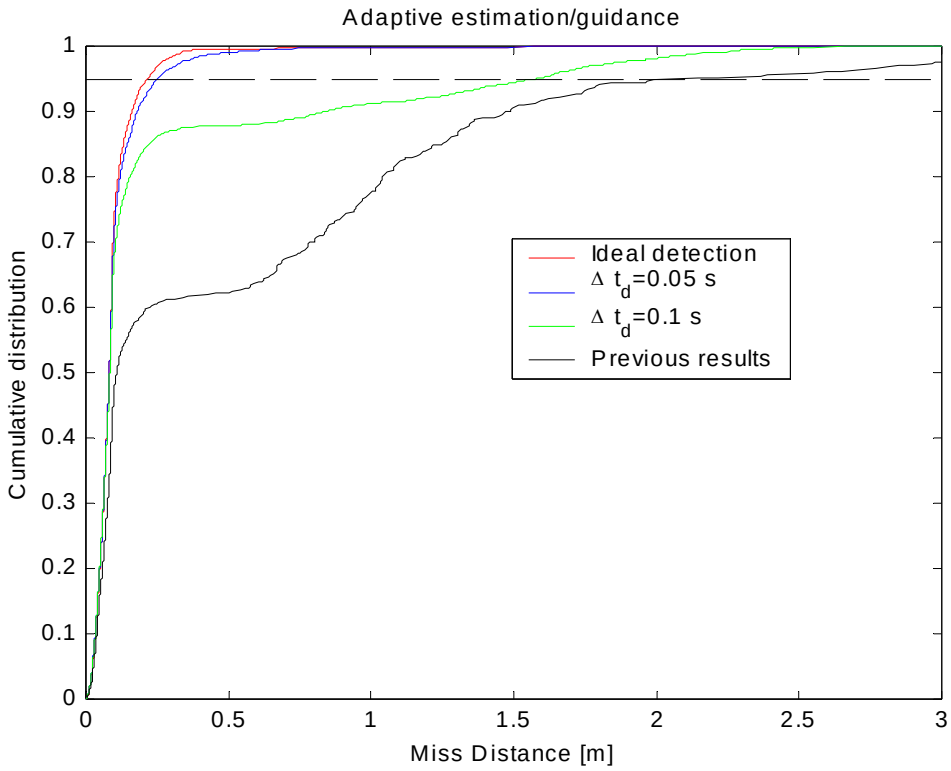

Fig. 7. Cumulative miss distance probability distribution against randomly switched "bang-bang" target maneuvers

While for a detection delay of Δt_d = 0.05 sec there was only a slight degradation of the homing performance, for Δt_d = 0.1 sec the degradation was more meaningful, mainly for maneuver switches near to the end of the interception. These results strongly emphasize the need for a fast "jump detector", which has to be developed. However, even in this case the improvement of the homing performance

compared to earlier results is substantial, as seen in Table 2, presenting the average miss distance (r_{av}), the maximum miss distances for 95% and 99% of kill probabilities (r_{95}, r_{99}) and the kill probability for a warhead lethality radius of 0.5 m ($p_{0.5m}$).

Table 2: Homing performance summary

Δt_d [s]	r_{av} [m]	r_{95} [m]	r_{99} [m]	$p_{0.5m}$ [%]
0	0.095	0.22	0.34	99.6
0.05	0.10	0.25	0.50	99.1
0.1	0.25	1.57	2.21	87.9
ITR2	0.57	2.14	3.51	62.3

For periodical maneuvers the adaptive estimation/guidance strategy, as well as the homing performance, remained the same as reported in ITR2.

5.3 Third year (October 2003-September 2004)

5.3.1. ITR3. (October 2003-May 2004)

Encouraged by the performance improvement achieved in the previous year and acknowledging the uncertainty about the practical value of the “jump” detection delay, the new approach of *logic based integrated estimation/ guidance algorithm* (as it was called in the sequel) was redefined using a system viewpoint. It was decided that since no single estimator can satisfy the requirements of homing accuracy, the different tasks performed by a classical estimator have to be separated and assigned to different elements within a corporate estimation system.

The main task, directly affecting the homing accuracy, is the *estimation of the state variables* (including the target acceleration) involved in the guidance law. This task can be performed in a satisfactory manner by a narrow bandwidth filter, if (and only if) the correct model of the target maneuver is available. Thus, the first task to be carried out (at the beginning of the endgame) is *model identification* using a multiple model structure [44]. The filters for this task should be of a large bandwidth, to be able performing fast *model identification*.

In a planar scenario a random "bang-bang" type maneuver is the most effective for evasion, thus the "model" has to include the direction of the current target acceleration. Moreover, another (large bandwidth) estimator has to perform the *detection of the direction reversal* (switch) that is anticipated. This is an additional task that requires a special estimator, which has to be developed.

If the "jump" occurs sufficiently far away from the end of the interception, there is sufficient time for the low bandwidth filter to converge and provide the correct new value to the guidance law. Thus, if an early "jump" has been detected fast enough, the low bandwidth state estimator can be maintained. As was shown by the red curve on the Fig. 3, the guidance law DGL/1 using the correct value of the target acceleration achieves small miss distances. However, if the "jump" occurs near the end very large miss distance is created due to the estimation delay.

In an earlier paper [45] a multiple model estimator, where each model assumed a different timing of the switch, was described. Using such an estimator "tuned" to the correct switch, e. g. $(t_{go})_{sw}$ = 1.0 s, eliminates the delay and yields

excellent homing performance as can be seen in Fig. 8 from the cumulative probability distribution of the miss distances obtained from 100 Monte Carlo runs. The robustness of such "tuned" estimators was already shown in Fig. 6.

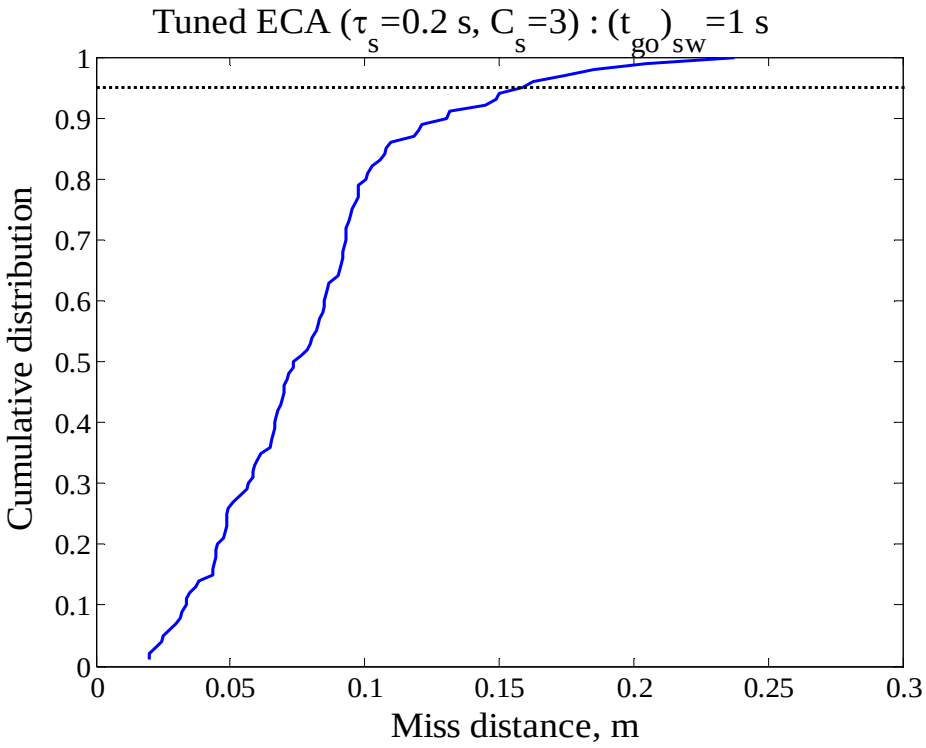

Fig. 8. Cumulative miss distance distribution of DGL/1 with a perfectly "tuned" estimator

Based on the results shown in Figs. 3 and 8, the following *logic based estimation/guidance strategy* was defined as an explicit function of the time-to-go:

1, At the beginning of the endgame (after achieving a "lock-on" the target) a multiple model estimator identifies whether the target maneuver is either quasi-constant or time varying (most probably periodical). During this identification period guidance is carried out by DGL/0.

2a, If a quasi-constant maneuver was identified, the next step is determining the maneuver direction and its (rough) magnitude.

2b, If a time varying maneuver was identified, assuming that is a part of a periodical maneuver, the next step is determining the frequency range.

2c, After the identification of the maneuver direction or the frequency range of the assumed periodical maneuver, the appropriate narrow band state estimator (ECA or PSF) is selected for state estimation and the guidance is carried out by DGL/1.

2d, In the case of quasi-constant maneuvers a special (fast) “jump” detection filter is used in parallel with the narrow bandwidth (ECA) state estimator.

3, If a “jump” has been detected before the critical time-to-go, the narrow bandwidth estimator is kept until the end. If a “jump” has been detected at or after the critical time-to-go, the narrow bandwidth estimator is replaced by the nearest (earlier) “tuned” wide bandwidth version (ECA) state estimator.

The simulation results obtained by using this *logic based integrated estimation/ guidance algorithm* without the "jump" detection filter, which has not been yet developed, were plotted in Fig.7 for several (assumed) detection delays (0, 0.05, 0.1 sec). In spite of the substantial improvement compared to earlier results, the homing performance in the case of 0.1 sec detection delay is not yet satisfactory. It was observed that if the "jump" occurs during the last phase of the interception, the interceptor is unable to reach its maximum lateral acceleration in the remaining short time and to correct the guidance error generated during the detection delay.

This deficiency was corrected by two intuitive modifications of the guidance law. The first one was based on increasing the lateral acceleration command, when a

maximum maneuver is needed due to the detected change of the target maneuver direction, for small values of time-to-go ($t_{go} < 3\tau_P$). The increase in the commanded acceleration gain is expressed for $t_{go} \le (t_{go})_{sw}$ by

$$a_p^c = a_p^c(t_{go}, k) = \frac{a_p^{\max} \operatorname{sign} Z}{1 - k \exp\left(-t_{go}/\tau_P\right)}. \tag{25}$$

where the parameter k is selected to satisfy

$$|a_p(t_f, k)| = a_P^{\max}. \tag{26}$$

Its value, which must be less than 1, otherwise the gain will be infinite, depends on $(t_{go})_{sw}$ and the value of a_P at that very moment.

The second modification was to replace the sign function in the DGL/1 guidance law within the period when the "tuned" estimators are used by a time varying dead zone version

$$\operatorname{sign}_{dz}(Z) = \begin{cases} 1.0, & Z > A_{dz} \exp(-b_{dz}(t_f - t_{go})), \\ 0.0, & |Z| \le A_{dz} \exp(-b_{dz}(t_f - t_{go})), \\ -1.0, & Z < -A_{dz} \exp(-b_{dz}(t_f - t_{go})), \end{cases} \tag{27}$$

where A_{dz} is the initial amplitude and b_{dz} is exponential decay rate of the dead zone. This modification reduces the error created during the period of estimation delay as illustrated in Fig. 9. The dead zone was used only in the interval 1.0 s > t_{go} > 0.2 s until the switch is detected. In the simulations the values of A_{dz} = 50 m and b_{dz} = 1/s were selected.

By applying both modifications (25) and (27) the homing performance is indeed improved, as can be clearly seen in the cumulative distributions in Fig. 10.

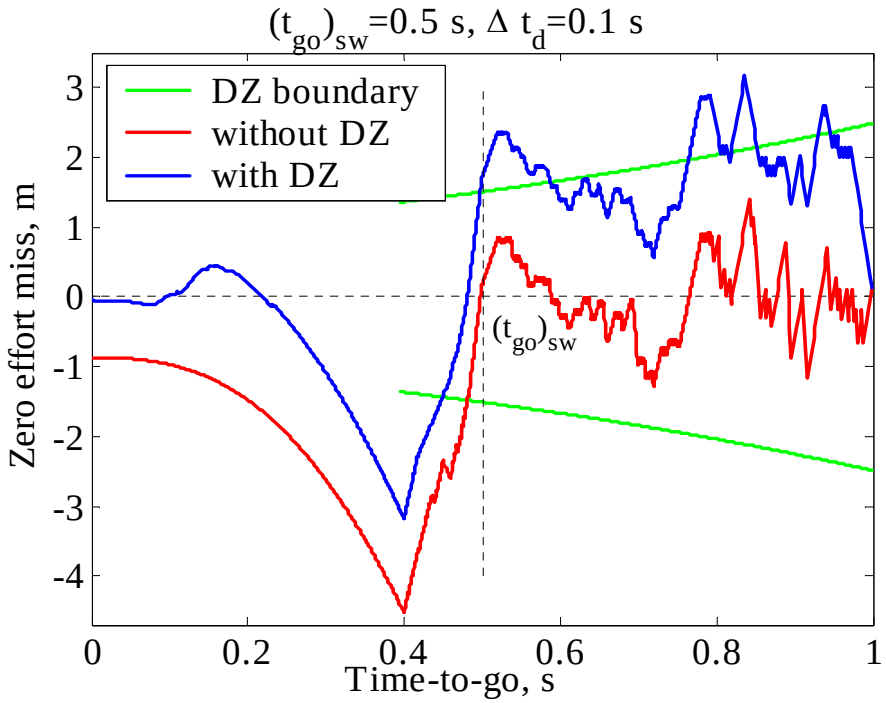

Fig. 9. The effect of time-varying dead zone

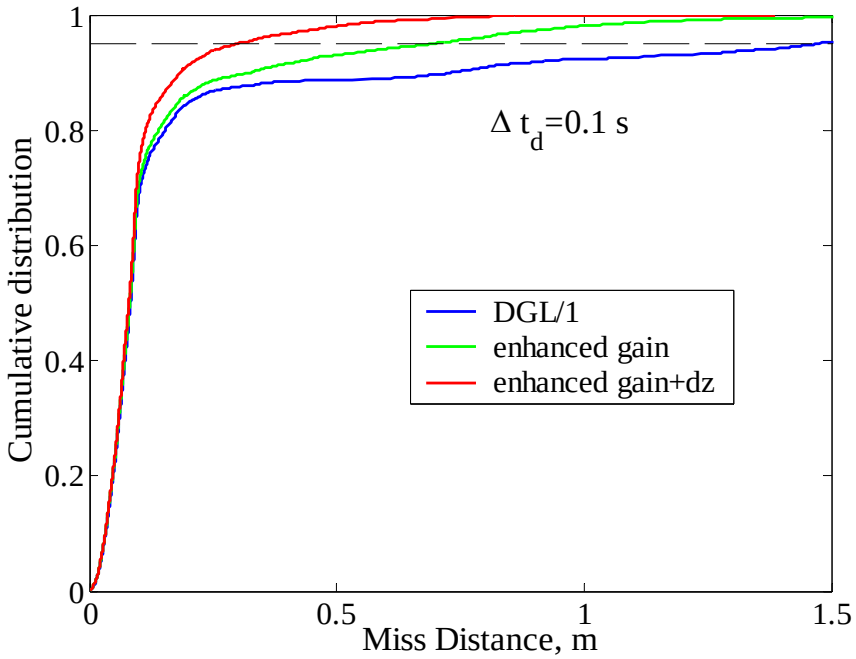

Fig. 10. Cumulative miss distance distributions with guidance law modifications

In Table 3 different figures of merit for the homing performance (the average miss distance r_{av}, the maximum miss distance for 95% of kill probability r_{95}, as well as $p_{0.5m}$, the kill probability for a warhead lethality radius of 0.5 m) of the horizontal constant speed interception endgame are summarized.

Table 3. Horizontal homing performance summary

Δt_d [s]	$r_{av,}$ [m]	$r_{95,}$ [m]	$p_{0.5m}$, [%]
0	0.095	0.22	99.6
0.05	0.10	0.25	99.1
0.1	0.23	1.47	88.5
0.1 & k	0.15	0.69	93.1
0.1 & k + dz	0.10	0.30	98.1
ITR2	0.57	2.14	62.3

The *new logic based estimation/guidance strategy* outlined above (with increased terminal gain and dead-zone) was also tested in a generic three-dimensional endo-atmospheric BMD scenario. The description and the data base of such scenarios are given in Appendix D. It was a nominal point defense scenario with a desired interception altitude of the 20 km. The target was a cruciform tactical ballistic missile aerodynamically controllable in pitch and roll that can perform either horizontal or "spiral" maneuvers. The interceptor was a cruciform aerodynamically controlled and roll-stabilized missile with solid rocket propulsion of two stages. Its maneuverability was limited by the maximum lift coefficient. The homing endgame stared at a slant range of 20 km and the guidance laws were adapted to time varying parameters (DGL/E instead of DGL/1). The results, shown in Fig.11 and Table 4, indicate

similarly improved homing performance, as a function of the detection delay. These results were also presented at two conferences [30,31].

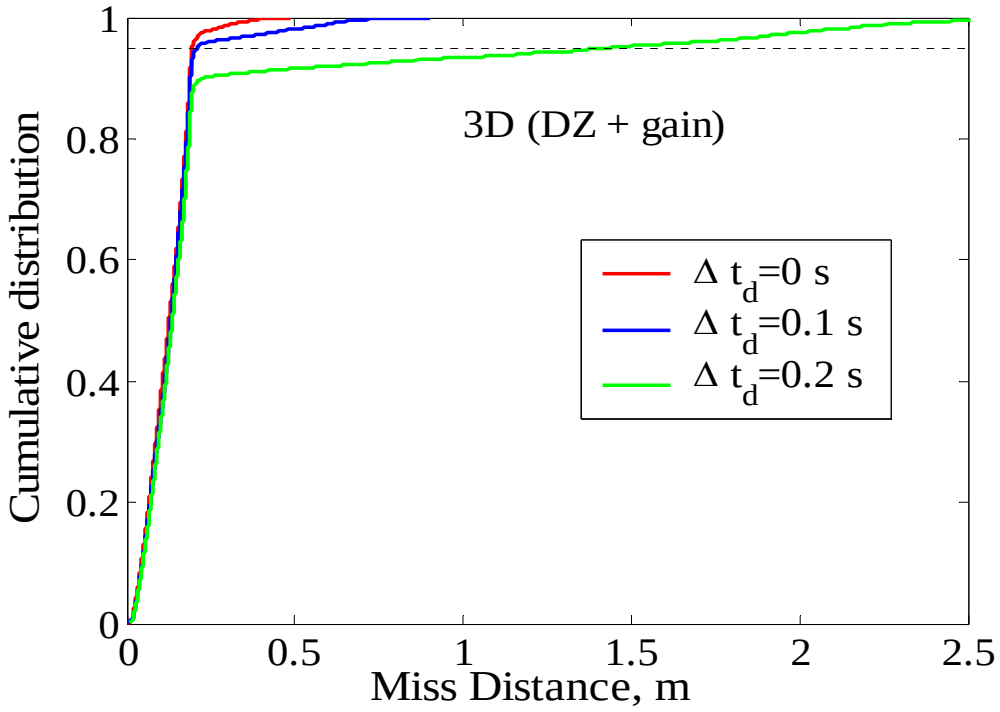

Fig. 11. Cumulative miss distance distributions in a three-dimensional interception

Table 4. Three-dimensional homing performance summary

$\Delta t_{d,}$ [s]	r_{av}, [m]	$R_{95,}$ [m]	$P_{0.5m,}$ [%]
0	0.12	0.20	99.8
0.1	0.14	0.21	98.1
0.2	0.25	1.43	91.6

The above presented results demonstrated that applying the new *integrated logic based estimation/guidance algorithm* in generic interception scenarios against

randomly maneuvering targets a substantial homing performance improvement was achieved, compared to earlier results. The new approach also has a potential to satisfy a “hit-to-kill” requirement against the most efficient "bang-bang" type maneuvers.

Against "spiral" (periodical) maneuvers the homing performance is even better. The crucial element for the successful application of the new algorithm is the existence of a sufficiently fast “jump” detector. The development of such a detector was not included in the original research program and it has to be the subject of an eventual future investigation.

5.3.2. (June- September 2004)

The results of the investigations performed in the last months of the contract and have not yet been reported are presented in the next section.

6. Recent results

The investigation efforts of the last months of the contract concentrated on validating the *logic based integrated estimation/ guidance algorithm*, developed using a planar constant speed interception endgame model, in several generic three-dimensional endo-atmospheric BMD scenarios. As mentioned earlier, the database for the simulation of such scenarios is given in Appendix D. The general description of this scenario is presented in the following subsection.

6.1. Three-dimensional BMD scenario description

The investigated interception scenario is an endgame between an interceptor missile launched against a maneuverable reentering tactical ballistic missile (TBM). For the sake of simplicity a nominal *point defense* scenario is considered, *i.e.* the surface target of the TBM is located in the vicinity of interceptor missile's launch site. It is assumed that the TBM is launched from the range of 600 km on a minimum energy trajectory. It is detected in its reentry phase at the altitude of 150 km (slant range of 258 km, velocity of 1720 m/s and a flight path angle of -18.2^{o}). The detailed simulation of the TBM reentry trajectory starts with these initial conditions on a nominal (non maneuvering) target trajectory.

The TBM is a generic cruciform flying vehicle having aerodynamic control surfaces that can execute lateral maneuvers up to a given angle of attack in fixed (non-rolling) body coordinates. The simulation of the TBM motion is of 4 degrees of freedom, including in addition to the point-mass model also a rolling motion around the velocity vector. Due to eventual (or planned) lateral asymmetry, the reentering TBM also rotates (rolls) about its longitudinal axis and (having a non-zero trim angle of attack) follows a "spiral" type trajectory. However, it can also be roll stabilized, performing maneuvers in a predetermined plane. The TBM is characterized by its ballistic coefficient, which determines the deceleration in the atmosphere and the lift to drag ratio at the trimmed angle of attack generating lift and the parameters of the rolling motion. These parameters are defined in Appendix D.

The generic interceptor missile (designed by a group of students for high endo-atmospheric interception) has an aerodynamically controlled cruciform airframe

and is assumed to be roll stabilized. It has solid rocket propulsion of two stages. Each rocket motor stage provides a constant thrust. After the “burn out” of the first stage the booster is separated and the second rocket motor is ignited. The ignition of the second propulsion stage is delayed to allow maximum interceptor velocity at the end of the interception. The maneuverability of the missile (its lateral acceleration and the corresponding load factor) is limited, in each of the two perpendicular planes of the cruciform configuration, by the maximum lift coefficient. The interceptor's aerodynamic and propulsion data are presented in Appendix D.

6.2. Midcourse precomputation

When the TBM is detected, the defense system selects the desired altitude for interception and launches a guided missile towards the predicted point of impact at this altitude. In order to intercept the “nominal” target at the desired altitude a subprogram calculates the time of launching and the initial flight path angle of the interceptor. It also computes the appropriate delay for the ignition of the second stage rocket motor in order to maximize the interceptor velocity at the nominal interception altitude. The interceptor is launched according to the precomputed results of the subprogram and guided from the ground to reach the “nominal” interception point until the “lock-on” range of the interceptor’s seeker is reached. During that time the target trajectory is simulated, allowing also eventual maneuvers. Due to the differences between the precomputed (“nominal”) and the simulated (“real”) trajectories, the initial conditions of the interception end game are not “ideal” and the endgame starts with some initial error, as can be expected in reality.

6.3. Three-dimensional endgame simulations

It is assumed that the homing endgame starts at a slant range of 20 km. Based on the available data the “nominal” velocity and maneuverability profiles of the interceptor and the TBM during the endgame, as well as the time varying interceptor/target maneuverability ratio μ can be computed, as shown in Figs. D.5-D.7 in Appendix D for a nominal interception altitude of 20 km. It can be seen in Fig. D.7 that during the endgame the maneuverability ratio μ, characterizing the interceptor advantage, is monotonically (almost linearly) decreasing. The entire endgame can be characterized by the final value of this parameter, denoted as μ_f.

Three scenarios with different interception altitudes (20, 25 ,30 km) were simulated. Results obtained in earlier studies showed that randomly switched "bang-bang" maneuvers are the most effective. Thus, it was assumed that the TBM is roll stabilized and the maneuvers are executed in the horizontal plane. As in earlier simulations, it was assumed that the endgame starts with a target maneuvering to the right and at some random time during the endgame a command of maneuver direction change is given. The relationship between the TBM’s actual angle of attack and its commanded value was approximated by a first-order transfer function with a time constant $\tau_p = 0.2$ sec.

The interceptor missile used during the endgame the *logic based estimation/guidance strategy* outlined in detail in the previous section, but the guidance law used is DGL/E which is adapted to the nominal time varying parameters of the endgame. The narrow bandwidth state ECA estimator used in the planar

simulations remained unchanged. The parameters of the 3 "tuned" wide bandwidth ECA state estimators (τ_s and C_s) were selected, based on a large set of Monte Carlo runs to optimize the homing performance. The interceptor's autopilot was represented by a first-order transfer function with a time constant τ_p = 0.2 sec, as in the planar simulations.

6.4. Simulation results

The fist step was to establish the parameters to be used for the selected interception scenarios, each aimed for a different altitude. The initial conditions of each scenario, obtained from the precomputations, are summarized in Appendix D, subsection D.3. The next step was to determine the parameters of the 3 "tuned" wide bandwidth ECA state estimators that optimize the homing performance for each nominal interception altitude. A very large set of Monte Carlo runs, composed of 1000 randomly selected maneuver switches during the endgame with independently selected noise sequences for every pair of fixed parameters (a total of 28000) were performed for each scenario. Based on these simulations it was established that within the framework of the *logic based integrated estimation/ guidance algorithm* the optimal homing performance is quite insensitive to the values of these parameters, indicating the robustness of the algorithm. The optimal parameters turned out to be practically the same as in the planar simulations (τ_s = 0.2 sec and C_s = 3). The homing performance measures are summarized in Table 5, where (due to the excellent homing performance) the kill probability for a warhead lethality radius of 0.3 m was used (instead of 0.5 m in Tables 3 and 4).

Table 4. Homing performance summary in three BMD scenarios

h_{int}, [km]	$r_{av,}$ [m]	$r_{95,}$ [m]	$p_{0.3m}$, [%]
20	0.14	0.21	96.0
25	0.13	0.21	99.5
30	0.20	0.30	94.6

The cumulative miss distance distributions of the different scenarios are presented in Fig.12.

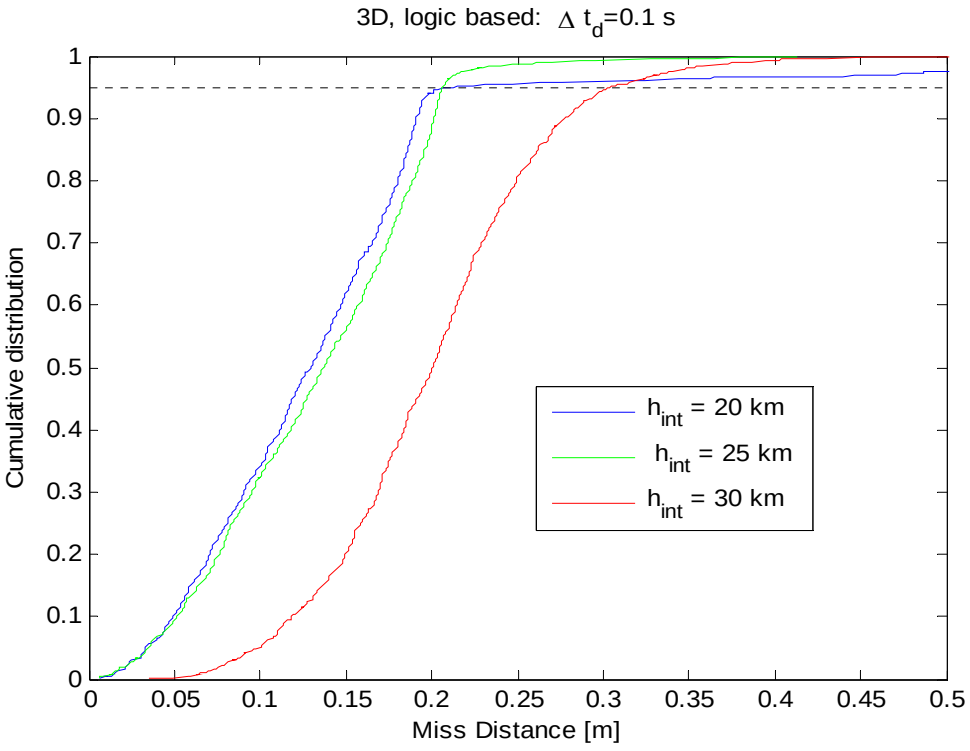

Fig. 12. Cumulative miss distance distributions three BMD scenarios

The results indicate a slightly better homing performance for 25 km than for 20 km, as well as some deterioration for an interception altitude of 30 km. These differences are probably due to the small differences in the maneuverability profiles of the scenarios.

In summary, one can say that using the *logic based integrated estimation/ guidance algorithm* the homing performance against randomly switched "bang-bang" maneuvers is uniformly excellent (almost "hit-to-kill") in the of lower tier endo-atmospheric interception altitude range of 20-30 km. The homing accuracy against random phase "spiral" maneuvers (as demonstrated earlier) is even better.

7. Concluding remarks

From the content of this Final Technical Report one can obtain a clear view of the progress made during the three years of the contract (No. F61775-01-C-0007). The need for an *integrated estimation/ guidance* was established and justified in the first phase. It was followed by a methodical investigation leading to the development of an innovative design approach for interceptor missiles using a *logic based integrated estimation/ guidance algorithm*. The algorithm was based on three new ideas:

1, Separation of the tasks of model identification, state reconstruction and abrupt change ("jump") detection and assigning each to different estimators.

2, Explicit use of the time-to-go to select the appropriate estimator for providing guidance information.

3, Modification of a differential game based bounded control guidance law (DGL/1) for enhancing its efficiency in the terminal phase.

The efficiency of the algorithm depends on the existence of a sufficiently fast "jump" detector. Since the development of such detector was not included in the

original research program, its performance (the detection delay) was parameterized in the simulations.

The results of extensive Monte Carlo simulations demonstrated an exceptional homing performance improvement (depending on the detection delay) against randomly switching "bang-bang" maneuvers, compared to earlier results, and an excellent robustness with respect to scenario parameters. The homing performance in the three-dimensional scenarios is somewhat better than in the planar case, due to the higher time varying interceptor maneuverability advantage. The miss distances against random phase "spiral" maneuvers (as demonstrated earlier) are even smaller.

Finally, a word of caution. The data used in the Monte Carlo simulations are generic and therefore the numerical results are only illustrative. However, the data represent a rather pessimistic case. In the planar engagement a non-excessive interceptor maneuverability advantage ($\mu = 2$), a relatively agile target ($\varepsilon = 1$) and a conservative sensor noise ($\sigma_{ang} = 0.1$ mrad) were assumed. The “bang-bang” target maneuver, used in the simulations, is the most efficient one for avoiding interception.

References

[1] Hughes, D., "Next Arrow Test this summer after Scoring Direct Hit", *Aviation Week & Space Technology*, March 24, 1997.

[2] Philips, H. E., "PAC-3 Missile Seeker Succeed" *Aviation Week & Space Technology*, March 22, 1999.

[3] Wall, R. "THAAD at Crossroads after Intercept" *Aviation Week & Space Technology*, August 9, 1999.

[4] Yuan, C. L., "Homing and Navigational Courses of Automatic Target Seeking Devices", *Journal of Applied Physics*, Vol. 19, No. 12, 1948, pp. 1122-1128.

[5] Kreindler, E., "Optimality of Proportional Navigation", *AIAA Journal*, Vol. 11, No. 6, 1973, pp. 878-880.

[6] Zarchan, P. *Tactical and Strategic Missile Guidance*, Vol. 124 in Progress in Astronautics and Aeronautics Series, 1990, AIAA, Inc. Washington D.C.

[7] Stengel, R. F. *Stochastic Optimal Control*, John Wiley & Sons, New York, 1986.

[8] Shinar, J. and Zarkh, M. "Interception of Maneuvering Tactical Ballistic Missiles in the Atmosphere", *Proceedings of the 19th ICAS Congress*, Anaheim, CA, 1994, pp.1354-1363.

[9] Shinar, J. and Shima, T., "Kill Probability Assessment against Maneuvering Tactical Ballistic Missiles", AIAA 10th Multinational Conference on Theater Missile Defense, Eilat, Israel, June 1997.

[10] Shinar, J., Shima, T. and Kebke, A. "Evaluation of Guidance Laws for the Interception of Highly Maneuvering Targets - Comparison to Linear Analysis", AIAA 11th Multinational Conference on Theater Missile Defense, Monterey CA, June 1998.

[12] Shinar, J. and Shima, T., "Towards Improved Guidance Laws against Highly Maneuvering Anti-Surface Missiles", 12th Multinational Conference on Theater Missile Defense Edinburgh, UK, 1 - 4 June, 1999.

[13] Shinar, J. and Shima, T., "Robust Missile Guidance Law against Highly Maneuvering Targets", *Proceedings of the 7th IEEE Mediterranean Conference on Control and Automation*, Haifa, Israel, 28-30 June 1999, pp.1548-1572.

[14] Shinar, J. and Glizer, V. Y. "Solution of a Delayed Information Linear Pursuit-Evasion Game with Bounded Controls" *International Game Theory Review*, Vol. 1, No. 3 & 4, 1999, pp. 197-218.

[15] J. Shinar and T. Shima, "On a Potential Breakthrough in Guidance Law Development for Intercepting Highly Maneuverable Ballistic Missiles" AIAA 13th Multinational Conference on Ballistic Missile Defense, Philadelphia, PA, June 2000.

[16] J. Shinar and T. Shima, "Non-orthodox Guidance Law Development Approach for the Interception of Maneuvering Anti-Surface Missiles", AIAA-2000-4273-CP AIAA Guidance, Navigation and Control Conference, Denver, CO, August 2000.

[17] J. Shinar and T. Shima, "Validation of an Improved Guidance Law for Intercepting Highly Maneuverable Ballistic Missiles", 2001 Multinational Conference on Ballistic Missile Defense, Maastricht, The Netherlands, June, 2001.

[18] J. Shinar, "On the Feasibility of "Hit-to-kill" in the Interception of Maneuvering Targets" invited paper, 2001 American Control Conference, Arlington, VA, 25-27 June 2001.

[19] T. Shima, J. Shinar and H. Weiss, "New Interceptor Guidance Law Integrating Time Varying and Estimation Delay Models", AIAA-2001-4344 CP, AIAA Guidance, Navigation and Control Conference, Montreal, Quebec, August 2001.

[20] Shima, T. and Shinar, J. (2002) "Time Varying Linear Pursuit-Evasion Game Models with Bounded Controls", *Journal of Guidance, Control and Dynamics*, Vol. 25, No.3, pp. 425-432.

[21] Shinar, J. and Shima, T., "Non-orthodox Guidance Law Development Approach for the Interception of Maneuvering Anti-Surface Missiles", *Journal of Guidance, Control and Dynamics*, Vol.25, No. 4, 2002, pp. 658-666.

[22] T. Shima, J. Shinar and H. Weiss, "New Interceptor Guidance Law Integrating Time Varying and Estimation Delay Models", *Journal of Guidance, Control and Dynamics*, Vol. 26, No. 2, 2003, pp. 295-303.

[23] J. Shinar and V. Turetsky, "On Improved Estimation for Interceptor Guidance**.**" invited paper, 2002 American Control Conference, Anchorage, Alaska, May 2002.

[24] J. Shinar, "The Estimation Challenge for Theatre Ballistic Missile Defense." 2002 Multinational Conference on Ballistic Missile Defense, Dallas, TX, June 2002.

[25] J. Shinar and V. Turetsky, "Interceptor Missile Guidance, - A Mature Science or a New Challenge?" invited paper, IFAC Congress, Barcelona, July 2002.

[26] J. Shinar, Y. Oshman, V. Turetsky and J. Evers, "On the Need for Integrated Estimation/Guidance Design for Hit-to-kill Accuracy", invited paper, 2003 American Control Conference, Denver, CO, June 2003.

[27] Shinar, J. and Turetsky, V., "What happens when certainty equivalence is not valid? -Is there an optimal estimator for terminal guidance?", *Annual Reviews in Control*, Volume 27, No. 2, 2003, pp. 119-254.

[28] J. Shinar, "On the Optimal Estimator of Randomly Maneuvering Targets for Terminal Guidance", 16th IFAC Symposium on Automatic Control in Aerospace, St. Petersburg, Russia, June, 2004.

[29] J. Shinar, "Error Reduction in Zero Effort Miss Distance Estimates for Improved Ballistic Missile Defense", 2004 Multinational Conference on Ballistic Missile Defense, Berlin, Germany, July 2004.

[30] J. Shinar, V. Turetsky, and Y. Oshman, "New Logic Based Estimation/Guidance Algorithm for Improved Homing Against Randomly Maneuvering Target", *Proceedings of AIAA Guidance, Navigation and Control Conference*, Providence, RI, August 2004.

[31] J. Evers, J. Shinar, V. Turetsky and Y. Oshman, "Integrated Estimator/Guidance Law Design for Improved Ballistic Missile Defense", AIAA Missile Science Conference, Monterrey, CA, November 2004.

[32] Shinar, J., and Turetsky, V. "Improved Estimation is a Prerequisite for Successful Terminal Guidance", will appear in Special Issue on Missile Guidance and Control, *Journal of Aerospace Engineering*, 2005.

[33] Shinar, J. "Solution Techniques for Realistic Pursuit-Evasion Games", in *Advances in Control and Dynamic Systems*, (C.T. Leondes, Ed.), Vol. 17, pp. 63-124, Academic Press, N.Y., 1981.

[34] Glizer, V. Y. and Shinar, J. “Optimal Evasion from a Pursuer with Delayed Information”, *Journal of Optimization Theory and Applications*, Vol.111, No. 1, 2001, pp. 7-38.

[35] Kalman, R.E. “A New Approach of Linear Filtering and Prediction Problems” *Trans. ASME,* Vol. 82D, 1960, pp.35-50

[36] Zarchan, P. Representation of Realistic Evasive Maneuvers by the Use of Shaping Filters, *Journal of Guidance and Control*, Vol. 2, No.1, 1979, pp. 290-295.

[37] Singer, R. A., "Estimating Optimal Filter Tracking Performance for Manned Maneuvering Targets", *IEEE Trans. on Aerospace and Electronic Systems,* Vol. ES-6, No. 4, 1970, pp. 473-483.

[38] Petrosjan, L. A. *"Differential Games of Pursuit"*, Series on Optimization, Vol. 2, pp. 169-177, World Scientific Publishing, Singapore, 1993.

[39] Rotstein, H. and Szneier, M., "An Exact Solution to the General 4-Blocks Discrete-Time Mixed H_2/H_∞ Problems via Convex Optimization" *IEEE Trans. Automatic Control,* Vol. AC-43, No. 6, 1998, pp. 1475-1480.

[40] Lai, T. L. and Shan, Z., "Efficient Recursive Algorithms for Detection of Abrupt Signal and Systems", *IEEE Trans. Automatic Control,* Vol. AC-44, No. 5, 1999, pp.

[41] Witsenhausen, H. S., "Separation of Estimation and Control for Discrete Time Systems," *Proceedings of the IEEE,* Vol. 59, No. 11, Nov. 1971, pp. 1557-1566.

[42] Shinar, J. and Turetsky, V., "On Improved Estimation for Interceptor Guidance**.**" *Proceedings of the 2002 American Control Conference*, Anchorage, Alaska, May 2002.

[43] Shinar, J., Oshman, Y., Turetsky, V., and Evers, J., "On the Need for Integrated Estimation/Guidance Design for Hit-to-kill Accuracy", *Proceedings of the 2003 American Control Conference*, Denver, CO, June 2003.

[44] Bar-Shalom, Y. and Xio-Rong, L., *"Estimation and Tracking: Principles, Techniques, and Software*", Artech House, 1993.

[45] Shima, T., Oshman, Y. and Shinar, J., "An Efficient Application of Multiple Model Adaptive Estimation in Ballistic Missile Interception Scenarios", *Journal of Guidance, Control and Dynamics,* Vol.25, No. 4, 2002, pp. 667-675.

[46] Gutman, S., "On Optimal Guidance for Homing Missiles", *Journal of Guidance and Control*, Vol. 3. No. 4, 1979. pp. 296-300.

[47] Shinar, J. and Gutman, S., "Three-Dimensional Optimal Pursuit and Evasion with Bounded Control", *IEEE Trans. on Automatic Control*, Vol. AC-25, No. 3, 1980, pp. 492-496.

[48] Weiss, H. and Hexner, G. “A Simple Structure for a High Performance 3-D Tracking Filter”, TAE 858, 2000.

[49] Hexner, G., Weiss, H and Dror, S., “Temporal Multiple Model Estimator for a Maneuvering Target”, TAE 864, 2001.

[50] Zarchan, P., “Proportional Navigation and Weaving Targets”, *Journal of Guidance, Control and Dynamics,* Vol. 18, No. 5, 1994, pp.969-974. .

Appendix A. Sections 6-7 ITR1/Part 2

A.1. Monte-Carlo simulation results

A.1.1. Effects of filter parameters

A.1.1.1. Estimation with ECA/SF

The values of r_{95} (in meters), obtained in the simulations for the **DGL/0** and **DGL/1** guidance laws with the KF-ECA/SF (Singer) estimator, are given in Tables A.1 & A.2. The accuracy of these results, based on estimating both the numerical integration error and the statistical error of the 95% percentile (due to the finite sample), is of order of ± 10 cm. For this reason the results are given with a single decimal digit.

Table A.1. Effect of ECA/SF parameters: DGL/0, σ_a=0.1 mrad, r_{95} [m]

τ_s, s \ C_s	1	2	3
0.2	4.6	5.0	5.7
0.4	4.0	3.8	4.5
0.6	3.8	3.6	4.4
0.8	3.7	3.7	4.5
1.0	3.6	3.7	4.5
1.5	3.6	3.7	4.5

Table A.2. Effect of ECA/SF parameters: DGL/1, σ_a=0.1 mrad, r_{95} [m]

τ_s, s \ C_s	1	2	3
0.2	3.2	3.8	4.6
0.4	4.4	4.5	5.1
0.6	5.0	5.1	5.8
0.8	5.3	5.6	6.4
1.0	5.5	5.9	6.7
1.5	5.9	6.4	7.3

It is seen that the influence of the filter time constant τ_s is different for each guidance law. For **DGL/1** the best result is provided by the minimal value of τ_s. For **DGL/0** the homing performance for small τ_s is the worst. With τ_s increasing it is slightly improves and stabilizes. This can be explained by the mutual effect of the estimation delay and bias. Increasing τ_s results in larger delay and smaller bias, but this influence is more serious in the estimate of the target acceleration in comparison with the estimate of the target velocity. For **DGL/1**, using the acceleration estimate, the effect of delay is more critical than the effect of bias. Therefore, the best results are obtained with this guidance law for the smallest value of τ_s. **DGL/0** takes into consideration only the velocity estimate and consequently the influence of τ_s is weaker. The effect of the coefficient C_s (the process noise standard deviation is given by $\sigma_s = a_E^{max}/C_s$) is similar but not identical for these two guidance laws. In the range of parameters considered in the report he value of r_{95} decreases monotonically with C_s decreasing.

A.1.1.2. Estimation with RST/SF

The values of r_{95} [m] with the RST/SF estimator for different values of the parameter C_r are summarized in Table A.3 and represented in Fig. A.1.

Table A.3. Effect of RST/SF parameter, σ_a=0.1 mrad, r_{95} [m]

C_r	r_{95} (DGL/0)	r_{95} (DGL/1)
2	3.4	6.7
4	4.4	5.9
6	5.0	5.2
8	5.8	5.4
10	6.3	6.3

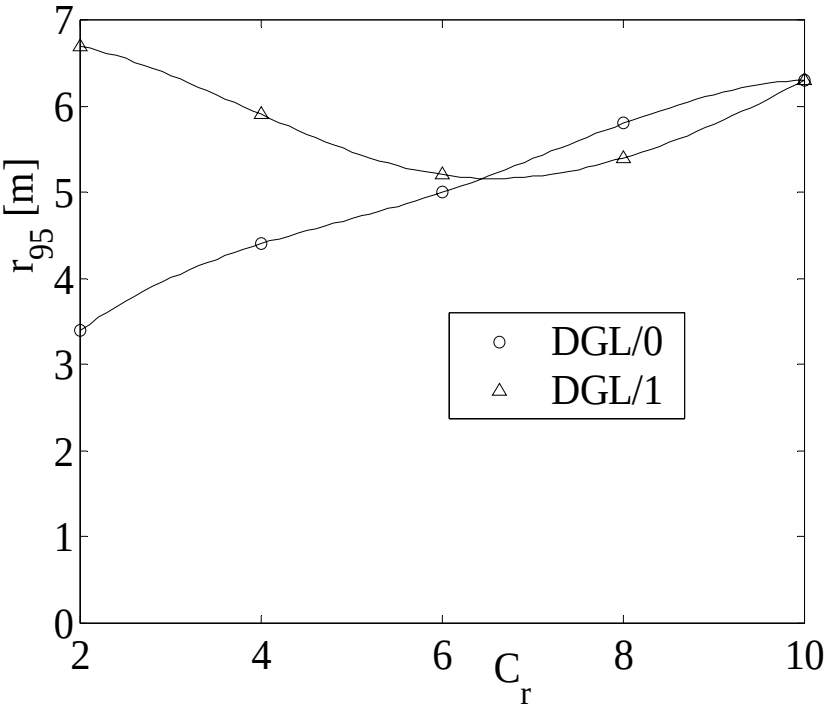

Fig. A.1. Effect of C_r (σ_a=0.1 mrad)

It is seen that for **DGL/0** the parameter C_r affects on the guidance result monotonically: the best result is provided by the smallest value of C_r. For **DGL/1** the graph "r_{95} vs. Cr" has a distinctive minimum, i.e. there exists an optimal value of C_r.

A.1.2. Comparison results

The cumulative distribution of the "worst" case miss distances (for a given estimator and guidance law combination) can be approximated as the sum of two parts: a "deterministic" minimal miss distance (r_m), due to the partially compensated estimation delay and of a random variable with a Rayleigh type probability distribution. Such distribution is characterized by a single parameter (b), which can be associated with the variance of the residual (converged) estimation error. Both values are monotonic functions of the measurement noise variance, depending on the estimator model and its parameters.

The best homing performance using **DGL/0**, the guidance law that does not require the knowledge of the target lateral acceleration, was achieved by using a KF-RST/SF estimator for both noise levels as it can be seen from Table A.4, where the respective tuning parameters of each estimator are also indicated.

Table A.4. Best results for DGL/0

Estimator	r_{95} [m]	r_{av} [m]	r_m [m]	b [m]
σ_a=0.1 mrad				
ECA, τ_s=0.6 s, C_S=0.5	3.6	2.9	2.1	0.6
RST, C_r=2	3.4	2.5	1.6	0.7
σ_a=0.2 mrad				
ECA, τ_s=0.5 s, C_S=0.5	7.0	5.4	3.7	1.3
RST, C_r=2	5.8	4.0	2.2	1.5

Using **DGL/1**, the guidance law that fully applies the target lateral acceleration in its implementation, the best homing performance was achieved by using a KF-ECA/SF estimator with a very small time constant τ_s = 0.2 sec, as it can be seen from Table A.5.

Table A.5. Best results for DGL/1

Estimator	r_{95} [m]	r_{av} [m]	r_m [m]	b [m]
σ_a=0.1 mrad				
ECA, τ_s=0.2 s, C_S=1	3.2	2.1	1.1	0.8
RST, C_r=6	5.2	3.2	1.0	1.8
σ_a=0.2 mrad				
ECA, τ_s=0.2 s, C_S=0.5	7.3	5.8	4.0	1.3
RST, C_r=8	9.1	5.5	2.0	2.8

The relative grading of the best homing performance of the delay compensating guidance law **DGL/C** with the different estimators is similar to the one with **DGL/0**. The results, summarized in Table A.6, also include the value of the (constant) estimation delay compensated by the guidance law. It can be also seen that the homing performance with each type of estimator is better than those achieved than by the other two guidance laws.

Table A.6. Best results for DGL/C

Estimator	r_{95} [m]	r_{av} [m]	r_m [m]	b [m]
σ_a=0.1 mrad				
ECA, τ_s=0.4 s, C_S=1, τ_{comp}=0.2 s	3.1	2.2	1.4	0.7
RST, C_r=2, τ_{comp}=0.45 s	3.1	2.1	1.2	0.7
σ_a=0.2 mrad				
ECA, τ_s=0.4 s, C_s=0.5, τ_{comp}=0.2 s	5.8	3.9	2	1.5
RST, C_r=2, τ_{comp}=1 s	5.9	4.0	2.2	1.5

A.2. Discussion

The numerical results presented in the previous section reveal several important phenomena. First, it is demonstrated experimentally that for the interception end game against a maneuvering target the Certainty Equivalence property and the associated Separation Theorem do not apply. The structure of the best estimator and its parameters strongly depend on the guidance law, as well as on the level of the measurement noise. Moreover, the relationship between the estimation performance and homing performance is less than obvious. This becomes clear in the cases of **DGL/0** and **DGL/1**, which are uniquely defined guidance laws.

The sensitivity of **DGL/0** to the estimator delay is minimal, because this guidance law doesn't include the target acceleration in the *zero effort miss distance*. However, it is strongly affected by a biased estimate of the relative lateral velocity. This is the reason that when using this guidance law, the KF-RST/SF estimator is superior to KF-ECA/SF. Moreover, the best KF-ECA/SF for this case has a relatively large time constant (τ_s=0.6 s) in order to reduce the bias on the expense of a larger estimation delay.

In the case of **DGL/1**, the guidance law that fully accounts for the target acceleration, the situation is entirely different. Due to the high sensitivity of this guidance law to the estimation delay, the best estimator is a KF-ECA/SF with a small time constant (τ_s=0.2 s) in spite of its large negative bias. A reason for the relatively good homing performance is the "bang-bang" type guidance law implementation. As long as the sign of the *zero effort miss distance* doesn't change, even if its absolute value is incorrect, the guidance command remains the same. Another possible reason may be that the effects of the estimation delay and of the negative bias the homing performance tend to weaken each other.

The situation with the guidance law **DGL/C** is extremely complex. In this case there is a strong interaction between the parameters of the estimator and τ_{comp}, the delay compensation time of the guidance law. For a given set of tuning parameters of the estimator the best value of τ_{comp} can be found. However, the very value of τ_{comp} effects the selection of the best tuning parameters for a given estimator structure. Finding the best combination requires a simultaneous search in the joint estimator/guidance law parameter space. It is also observed that using **DGL/C** the

difference between the homing performances of the various estimators is much smaller than with the other guidance laws, as it can be seen in Fig. A.2. **DGL/C** seems to correct, at least partially, the deficiencies of the estimators.

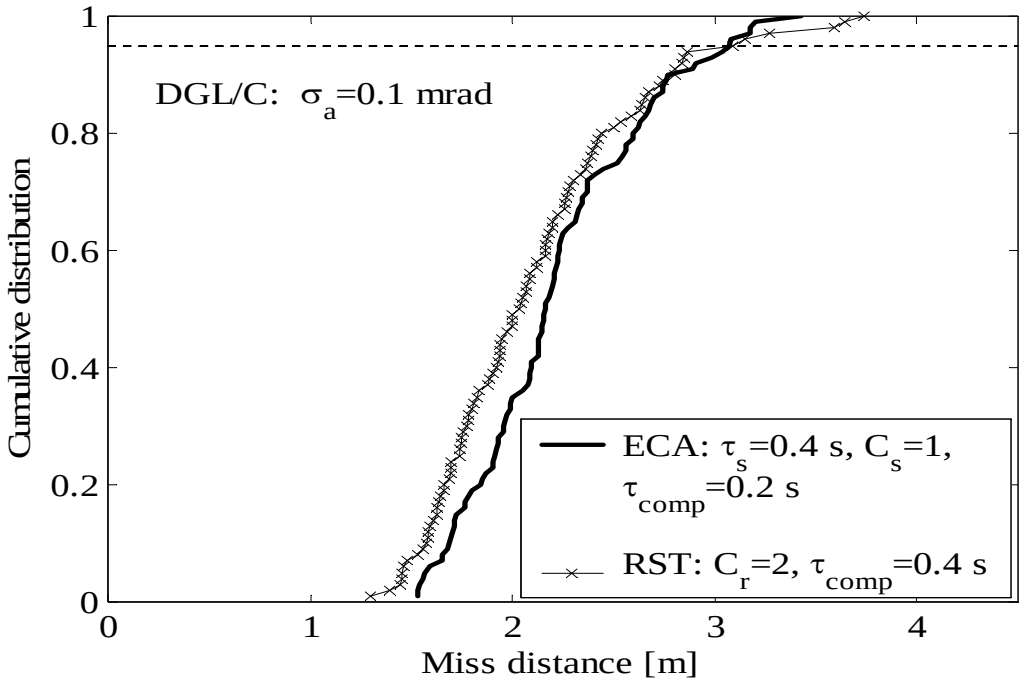

Fig. A.2. Worst case performance comparison with different estimators

Another unexpected phenomenon is the unclear relationship between actual estimation delay in detecting a change in lateral target acceleration, as it is measured from the ensemble average of the estimator data, and the best value of τ_{comp} used in the guidance law. The best value of τ_{comp} doesn't have either a direct relationship with the predicted value of the minimum time needed to detect target maneuver change [16]. This delay is of the order of 0.25 sec for smaller noise level (σ_a=0.1 mrad) and of the order of 0.34 sec for σ_a=0.2 mrad.

The source of these surprising results is most probably in the rough approximation of the estimation process made during the development of the guidance law [8, 14], assuming that the "evader's lateral acceleration is a perfect outcome delayed by the amount of Δt_{est}, while the estimation of the other state variables is ideal".

From the ensemble average of the estimator data one can observe that there is also a delay in the estimated relative lateral velocity. Moreover, the estimation delay of this state variable is not the same as the estimation delay of the lateral target acceleration and neither of these delays remains constant during the end game.

The results of the study also make clear the relation ship between the three differential game based guidance laws. **DGL/0** and **DGL/1** represent two extreme cases. In **DGL/0** the lateral target acceleration is not used in the guidance law, while **DGL/1** fully takes account of it. Depending on the noise level and the estimator structure, one of them has a better guaranteed (worst case) homing performance. Low noise level and large bandwidth estimator favor **DGL/1**, while in higher noise and using a small bandwidth estimator **DGL/0** is superior. The homing performance of **DGL/C** is always the best, but the amount of improvement contributed by its implementation depends on the noise level and the estimator. For high noise level the delay to be compensated is important and as a consequence the homing performance is not very different from that of **DGL/0** (see Fig. A.3). In a low level noise environment using a fast estimator (ECA, τ_s=0.2 s) only a small delay has to be compensated. Therefore, the homing performance of **DGL/C** will be only slightly superior to that of **DGL/1**, as it can be se+en from the numerical results in Tables A.4- A.6.

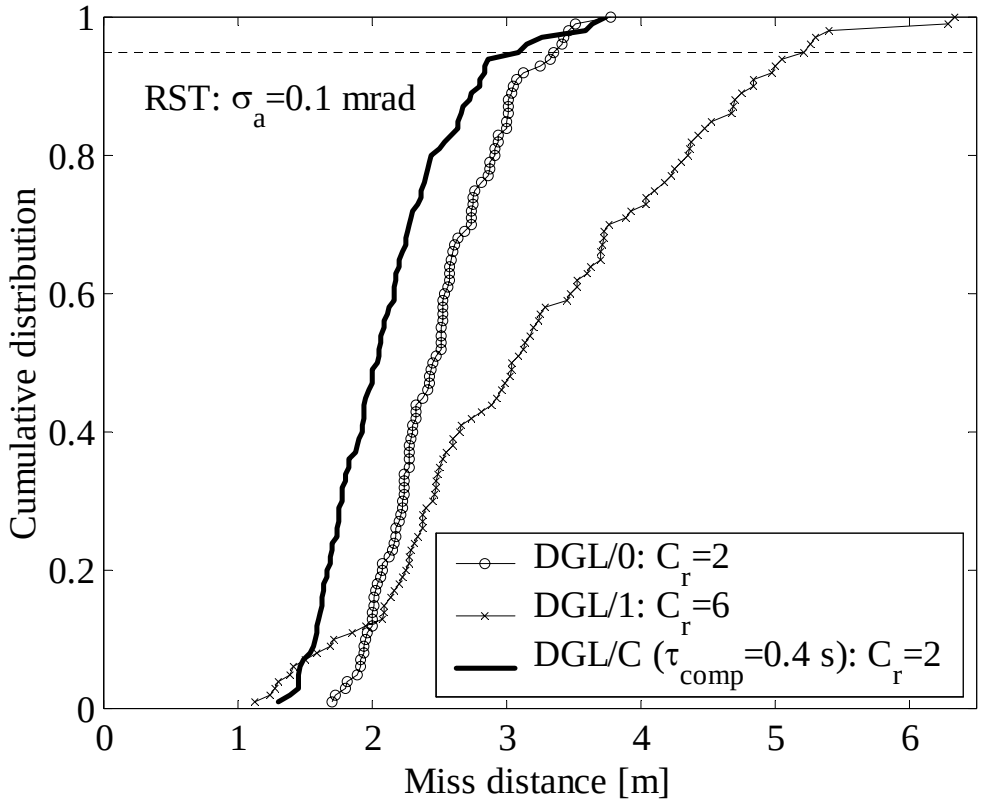

Fig A.3. Worst case homing performance of different guidance laws

Appendix B. Section 6 of ATR1

Based on the earlier results, summarized in subsection 5.1.1, as well as the results of a previous study conducted under AFOSR contract No. F61775-01-WE018, the new set of Monte Carlo simulations were oriented to test and compare the homing performance of several estimator/guidance law combinations with different maneuverability ratios ($1.5 \leq \mu \leq 3.0$) and two measurement noise levels ($\sigma_a = 0.1/0.2$ mrad) against two types of random target maneuvers:

(i) a "bang-bang" maneuver randomly switched during the interception end-game;

(ii) a sinusoidal maneuver with random phase, representing the planar projection of a three-dimensional "spiral" maneuver.

First, the results against "bang-bang" maneuvers were extended (from a single value of $\mu = 2$) to several values of maneuverability ratios using two well defined estimators (ECA with $\tau_s = 0.5$ sec and $C_s = 1$; RST with $C_r = 1$) and the guidance laws **DGL/1** and **DGL/C**. For each case the "worst" timing of the commanded direction change and the "best" value of delay compensation parameter τ_{comp} were determined and summarized in Tables B.1- B.4. The homing performance in these tables is characterized by the two numbers, the average miss distance of 100 Monte Carlo runs (r_{av}) and the value of a warhead lethality radius that guarantees an SSKP of 0.95 (r_{95}). The numerical accuracy of these results is estimated to be of the order of 0.1 m.

Table B.1. Bang-bang maneuver, DGL/1, RST

σ_a / μ	0.1 mrad			0.2 mrad		
	r_{95} [m]	r_{av} [m]	$(t_{go})_{sw}$ [s]	r_{95}	r_{av}	$(t_{go})_{sw}$ [s]
1.5	17.50	11.26	1.2	30.39	19.47	1.5
2.0	6.64	4.05	0.7	11.95	7.17	1.1
2.5	3.69	2.28	0.6	6.62	4.14	0.7
3.0	2.32	1.52	0.4	4.54	2.74	0.6

Table B.2. Bang-bang maneuver, DGL/1, ECA

σ_a / μ	0.1 mrad			0.2 mrad		
	r_{95} [m]	r_{av} [m]	$(t_{go})_{sw}$ [s]	r_{95}	r_{av}	$(t_{go})_{sw}$ [s]
1.5	11.73	7.96	1.1	20.20	13.69	1.4
2.0	4.42	2.81	0.7	7.48	4.87	0.9
2.5	2.36	1.43	0.5	4.16	2.77	0.6
3.0	1.69	1.08	0.4	3.08	1.79	0.6

Table B.3. Bang-bang maneuver, DGL/C, RST

σ_a / μ	0.1 mrad				0.2 mrad			
	Δt_{comp} [s]	r_{95} [m]	r_{av} [m]	$(t_{go})_{sw}$ [s]	τ_{comp} [s]	r_{95} [m]	r_{av} [m]	$(t_{go})_{sw}$ [s]
1.5	0.14	11.10	7.61	1.2	0.28	17.35	11.53	2.0
2.0	0.29	3.15	2.10	0.8	0.23	6.68	4.49	0.8
2.5	0.30	1.65	1.10	0.6	0.25	3.70	2.42	0.6
3.0	0.22	1.25	0.80	0.4	0.29	2.62	1.56	0.6

Table B.4. Bang-bang maneuver, DGL/C, ECA

σ_a / μ	0.1 mrad				0.2 mrad			
	Δt_{comp} [s]	r_{95} [m]	r_{av} [m]	$(t_{go})_{sw}$ [s]	τ_{comp} [s]	r_{95} [m]	r_{av} [m]	$(t_{go})_{sw}$ [s]
1.5	0.09	9.68	6.72	1.3	0.03	18.95	13.06	1.4
2.0	0.12	3.17	2.09	0.7	0.10	6.42	4.25	0.9
2.5	0.18	1.60	1.10	0.5	0.17	3.31	2.19	0.6
3.0	0.16	1.08	0.73	0.4	0.20	2.38	1.50	0.6

These results clearly confirm two expected trends, the strong improvement of homing performance with the increasing maneuverability ratio and its deterioration with increased noise. The sensitivities of each estimator/guidance law combination are, however, different. Between the two estimators the one with the ECA shaping filter provides better homing accuracy. The improvement of homing performance gained by the delay compensation of **DGL/C** is also evident. Considering these results as a base line for comparison, the great majority of the other simulations were made with sinusoidal random phase target maneuvers in the frequency band of ω = 1.0 - 7.0 rd/sec. The first group of Monte Carlo simulations with sinusoidal target maneuvers was performed against the four estimator/guidance law combinations used with "bang-bang" target maneuvers and for each case the "worst" phase was identified. The homing performance of these simulations is summarized in Tables B.5 – B.8. Comparison of the homing performance indicates that the miss distance against the "worst" sinusoidal target maneuver is always smaller than against the "worst" "bang-bang" maneuver. The reasons for the "reduced" effectiveness of a sinusoidal target maneuver are both the lower maneuver energy and the more gradual change, compared to the "bang-bang" maneuver of the same maximal amplitude.

Table B.5a. Sinusoidal maneuver, DGL/1, RST, σ_a = 0.1 mrad, r_{95} [m]

ω , rad/s / μ	0.5	1.0	1.5	2.0	2.5	3.0	3.5	5.0	7.5
1.5	2.12	2.67	3.33	4.33	4.61	5.02	5.30	5.15	3.08
2.0	0.76	0.96	1.29	1.49	1.85	2.11	2.51	2.78	2.45
2.5	0.47	0.57	0.67	0.84	1.08	1.23	1.34	1.76	1.81
3.0	0.39	0.45	0.52	0.65	0.73	0.82	0.91	1.25	1.37

Table B.5b. Sinusoidal maneuver, DGL/1, RST, σ_a = 0.1 mrad, r_{av} [m]

ω , rad/s / μ	0.5	1.0	1.5	2.0	2.5	3.0	3.5	5.0	7.5
1.5	1.08	1.32	1.72	2.23	2.68	3.08	3.36	3.20	2.03
2.0	0.33	0.43	0.57	0.78	1.01	1.24	1.44	1.77	1.53
2.5	0.20	0.25	0.32	0.42	0.54	0.65	0.75	0.99	1.03
3.0	0.15	0.19	0.23	0.29	0.34	0.42	0.50	0.68	0.77

Table B.5c. Sinusoidal maneuver, DGL/1, RST, σ_a = 0.2 mrad, r_{95} [m]

ω , rad/s / μ	0.5	1.0	1.5	2.0	2.5	3.0	3.5	5.0	7.5
1.5	3.90	5.41	7.18	8.45	8.81	9.39	9.47	7.54	4.08
2.0	1.50	1.83	2.56	3.20	3.73	4.36	4.99	5.25	3.68
2.0	0.91	1.22	1.41	1.82	2.17	2.55	2.91	3.53	3.11
3.0	0.82	0.96	1.18	1.37	1.64	1.73	2.00	2.55	2.51

Table B.5d. Sinusoidal maneuver, DGL/1, RST, σ_a = 0.2 mrad, r_{av} [m]

ω , rad/s / μ	0.5	1.0	1.5	2.0	2.5	3.0	3.5	5.0	7.5
1.5	2.12	2.74	3.64	4.56	5.31	5.74	5.83	4.51	2.44
2.0	0.66	0.93	1.27	1.71	2.16	2.60	2.93	3.20	2.26
2.5	0.36	0.48	0.68	0.92	1.18	1.45	1.70	2.15	1.86
3.0	0.26	0.35	0.47	0.62	0.78	0.93	1.10	1.43	1.41

Table B.6a. Sinusoidal maneuver, DGL/1, ECA, σ_a = 0.1 mrad, r_{95} [m]

ω , rad/s / μ	0.5	1.0	1.5	2.0	2.5	3.0	3.5	5.0	7.5
1.5	4.37	4.80	4.33	4.35	4.49	4.60	4.65	4.01	2.71
2.0	1.62	1.69	1.77	1.93	2.10	2.17	2.17	2.26	1.96
2.5	0.86	0.89	1.01	1.08	1.19	1.21	1.31	1.44	1.46
3.0	0.65	0.69	0.70	0.74	0.80	0.84	0.89	1.00	1.09

Table B.6b. Sinusoidal maneuver, DGL/1, ECA, σ_a = 0.1 mrad, r_{av} [m]

ω , rad/s / μ	0.5	1.0	1.5	2.0	2.5	3.0	3.5	5.0	7.5
1.5	2.57	2.69	2.79	2.87	2.93	2.94	2.92	2.65	2.65
2.0	0.86	0.90	0.99	1.10	1.18	1.27	1.36	1.41	1.41
2.5	0.47	0.49	0.55	0.59	0.65	0.70	0.76	0.85	0.85
3.0	0.31	0.33	0.35	0.38	0.42	0.47	0.50	0.59	0.59

Table B.6c. Sinusoidal maneuver, DGL/1, ECA, σ_a = 0.2 mrad, r_{95} [m]

ω , rad/s / μ	0.5	1.0	1.5	2.0	2.5	3.0	3.5	5.0	7.5
1.5	7.91	8.11	8.38	8.06	7.57	7.51	7.40	6.02	3.83
2.0	2.98	3.13	3.25	3.44	3.68	3.91	3.92	3.86	2.37
2.5	1.69	1.76	1.82	2.08	2.22	2.41	2.65	2.78	2.37
3.0	1.25	1.32	1.39	1.48	1.62	1.66	1.78	1.92	1.96

Table B.6d. Sinusoidal maneuver, DGL/1, ECA, σ_a = 0.2 mrad, r_{av} [m]

ω , rad/s / μ	0.5	1.0	1.5	2.0	2.5	3.0	3.5	5.0	7.5
1.5	4.91	5.03	5.08	5.08	4.98	4.92	4.78	4.00	2.32
2.0	1.76	1.88	2.00	2.16	2.34	2.48	2.56	2.54	1.96
2.5	0.94	0.98	1.09	1.20	1.30	1.43	1.54	1.67	1.47
3.0	0.63	0.67	0.73	0.80	0.88	0.94	1.01	1.14	1.54

Table B.7a. Sinusoidal maneuver, DGL/C, RST, σ_a = 0.1 mrad, r_{95} [m]

ω , rad/s / μ	0.5	1.0	1.5	2.0	2.5	3.0	3.5	5.0	7.5
1.5	5.12	4.99	4.62	4.58	4.62	4.64	4.56	3.78	2.60
2.0	2.67	2.67	2.64	2.45	2.41	2.37	2.31	1.97	1.54
2.5	1.52	1.52	1.47	1.50	1.48	1.42	1.44	1.33	1.12
3.0	0.93	0.92	0.94	0.95	0.95	0.99	0.97	0.97	0.95

Table B.7b. Sinusoidal maneuver, DGL/C, RST, σ_a = 0.1 mrad, r_{av} [m]

ω , rad/s / μ	0.5	1.0	1.5	2.0	2.5	3.0	3.5	5.0	7.5
1.5	3.08	3.11	3.13	3.11	3.09	3.02	2.89	2.52	1.78
2.0	1.82	1.82	1.78	1.69	1.63	1.59	1.51	1.28	0.99
2.5	1.00	0.99	0.95	0.97	0.94	0.91	0.90	0.83	0.70
3.0	0.56	0.55	0.57	0.57	0.57	0.58	0.57	0.58	0.55

Table B.7c. Sinusoidal maneuver, DGL/C, RST, σ_a = 0.2 mrad, r_{95} [m]

ω , rad/s / μ	0.5	1.0	1.5	2.0	2.5	3.0	3.5	5.0	7.5
1.5	8.90	9.03	8.46	8.21	7.67	7.13	6.82	6.13	3.82
2.0	3.44	3.53	3.60	3.71	3.69	3.73	3.75	3.42	2.67
2.5	2.06	2.12	2.14	2.23	2.38	2.39	2.42	2.43	2.05
3.0	1.62	1.61	1.66	1.68	1.72	1.78	1.77	1.85	1.89

Table B.7d. Sinusoidal maneuver, DGL/C, RST, σ_a = 0.2 mrad, r_{av} [m]

ω , rad/s / μ	0.5	1.0	1.5	2.0	2.5	3.0	3.5	5.0	7.5
1.5	5.81	5.81	5.63	5.45	5.14	4.85	4.61	4.01	2.32
2.0	2.24	2.32	2.38	2.41	2.46	2.53	2.54	2.31	1.75
2.5	1.29	1.32	1.34	1.43	1.48	1.50	1.54	1.50	1.27
3.0	0.91	0.91	0.95	0.98	0.99	1.04	1.05	1.09	1.08

Table B.8a. Sinusoidal maneuver, DGL/C, ECA, σ_a = 0.1 mrad, r_{95} [m]

ω , rad/s / μ	0.5	1.0	1.5	2.0	2.5	3.0	3.5	5.0	7.5
1.5	6.42	6.3	5.36	4.94	4.75	4.62	4.35	3.49	2.41
2.0	2.56	2.58	2.55	2.37	2.36	2.36	2.28	1.98	1.58
2.5	1.59	1.60	1.52	1.54	1.51	1.47	1.45	1.29	1.09
3.0	1.01	1.09	1.08	1.08	1.05	1.07	1.04	0.99	0.90

Table B.8b. Sinusoidal maneuver, DGL/C, ECA, σ_a = 0.1 mrad, r_{av} [m]

ω , rad/s / μ	0.5	1.0	1.5	2.0	2.5	3.0	3.5	5.0	7.5
1.5	4.07	3.94	3.68	3.45	3.31	3.14	2.93	2.38	1.66
2.0	1.70	1.70	1.67	1.60	1.57	1.54	1.47	1.28	1.01
2.5	1.07	1.07	1.02	1.02	0.99	0.94	0.93	0.84	0.69
3.0	0.69	0.68	0.67	0.67	0.64	0.65	0.63	0.59	0.53

Table B.8c. Sinusoidal maneuver, DGL/C, ECA, σ_a = 0.2 mrad, r_{95} [m]

ω , rad/s / μ	0.5	1.0	1.5	2.0	2.5	3.0	3.5	5.0	7.5
1.5	8.93	8.65	8.34	8.20	7.67	7.20	7.10	5.67	3.67
2.0	3.73	3.82	3.83	3.88	3.86	3.83	3.79	3.41	2.64
2.5	2.51	2.51	2.56	2.49	2.47	2.47	2.44	2.28	1.94
3.0	1.82	1.83	1.82	1.82	1.80	1.82	1.82	1.82	1.66

Table B.8d. Sinusoidal maneuver, DGL/C, ECA, σ_a = 0.2 mrad, r_{av} [m]

ω , rad/s / μ	0.5	1.0	1.5	2.0	2.5	3.0	3.5	5.0	7.5
1.5	5.58	5.56	5.45	5.31	5.06	4.87	4.67	3.88	2.29
2.0	2.55	2.60	2.62	2.61	2.56	2.56	2.54	2.30	1.73
2.5	1.68	1.70	1.67	1.65	1.66	1.64	1.58	1.48	1.21
3.0	1.16	1.16	1.13	1.16	1.15	1.12	1.13	1.08	0.98

The influence of different maneuver frequencies on the homing performance is shown in Fig. B.1 for $\mu = 2$, using the average miss distance of the "worst" case as a figure of merit. For other values of μ, the qualitative behavior is similar.

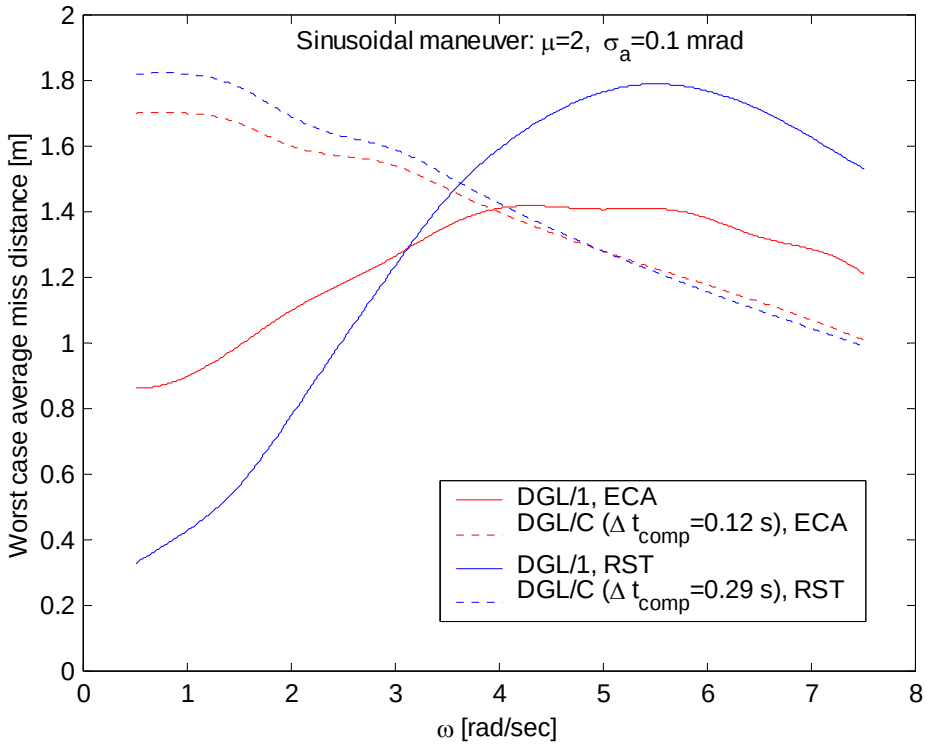

Fig. B.1. Influence of maneuver frequency

From these results several phenomena can be learned. The dependence of homing performance on the target maneuver frequency for the two different guidance laws is very different. Using DGL/1 there is a distinct maximum of the miss distance, i. e. a "worst" maneuver frequency, depending on the estimator. Moreover, for lower maneuver frequencies the RST estimator should be preferred, while for larger values of ω the ECA estimator yields better results. Using DGL/C the homing performance with both estimators is improving as the maneuver frequency increases. The difference between the two estimators is not significant, because this guidance law compensates for the deficiencies of both. The results also show that for the lower

maneuver frequencies DGL/1 is better, but for higher frequencies DGL/C provides guidance that is more accurate. The crossover frequencies between DGL/C and DGL/1, as well as between the two estimators with DGL/1 depend on the value of μ.

In spite of the fact that the miss distance against the "worst" sinusoidal target maneuver is always smaller than against the "worst" "bang-bang" maneuver, it has been quite obvious that neither the ECA nor the RST shaping filters are "ideal" for modeling periodical random phase maneuvers. In Fig. B.2 the actual lateral target acceleration is compared to the ensemble average of the one estimated by using an ECA shaping filter, exhibiting a substantial time varying delay.

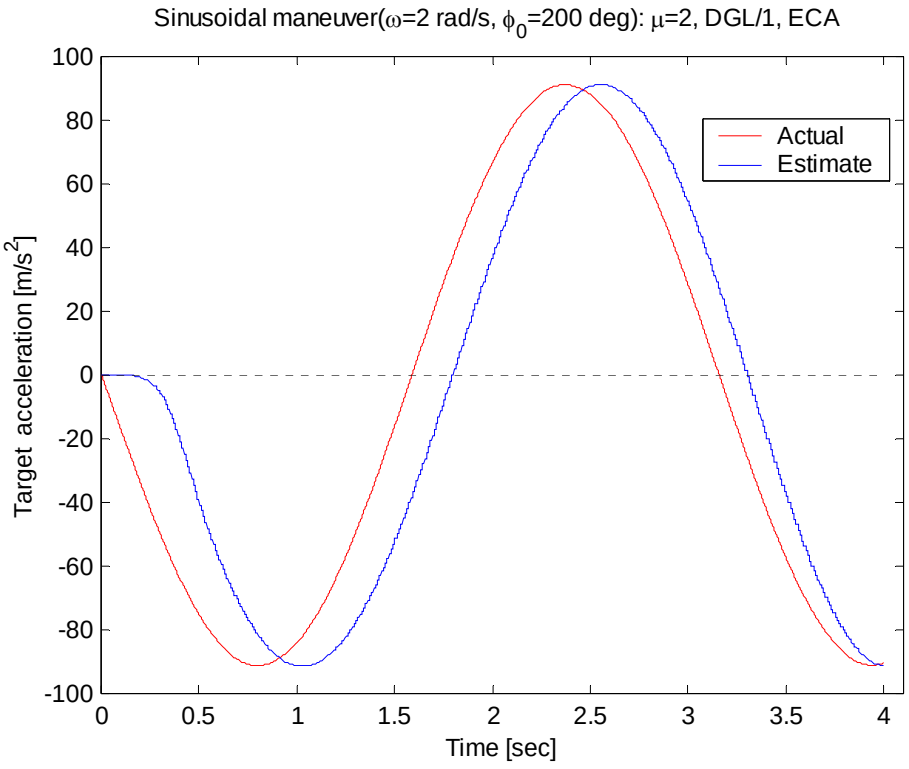

Fig. B.2. Estimation of target lateral acceleration with ECA

By replacing this shaping filter by one designed for a sinusoidal maneuver of a given frequency [36], denoted as PSF, one can obtain an "almost perfect" estimate, as shown in Fig. B.3. As a consequence substantially reduced miss distances are achieved.

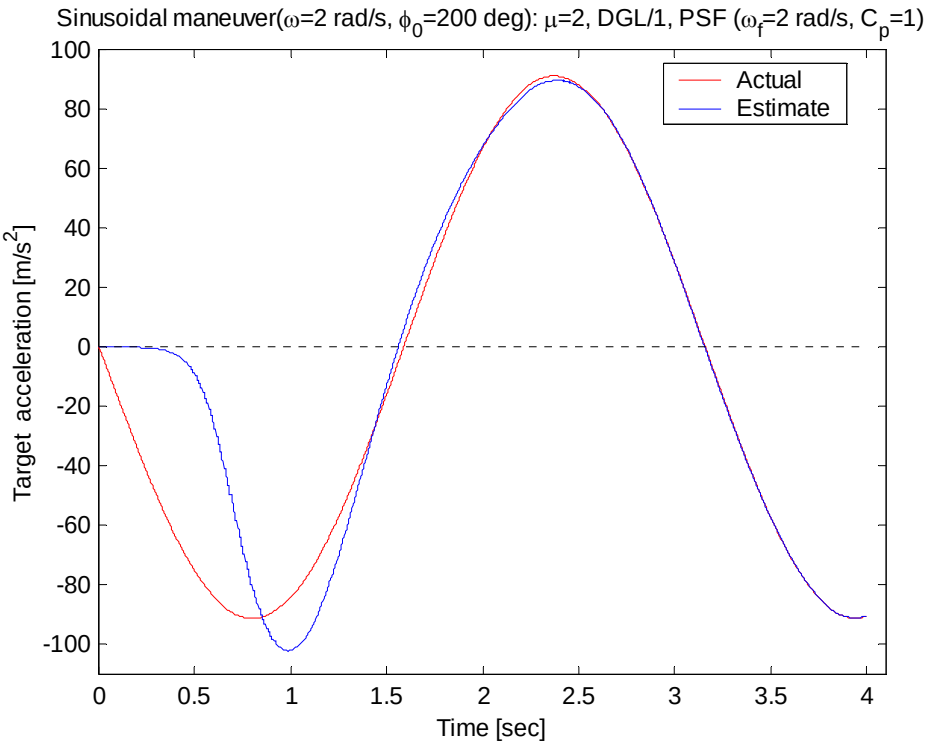

Fig. B.3. Estimation of target lateral acceleration with matched filter

If the assumed and actual frequencies don't match, the estimation performance deteriorates, as it is shown in Fig. B.4.

The consequence of the increased estimation errors is a deterioration of the homing performance, summarized in Tables B.9 – B.10.

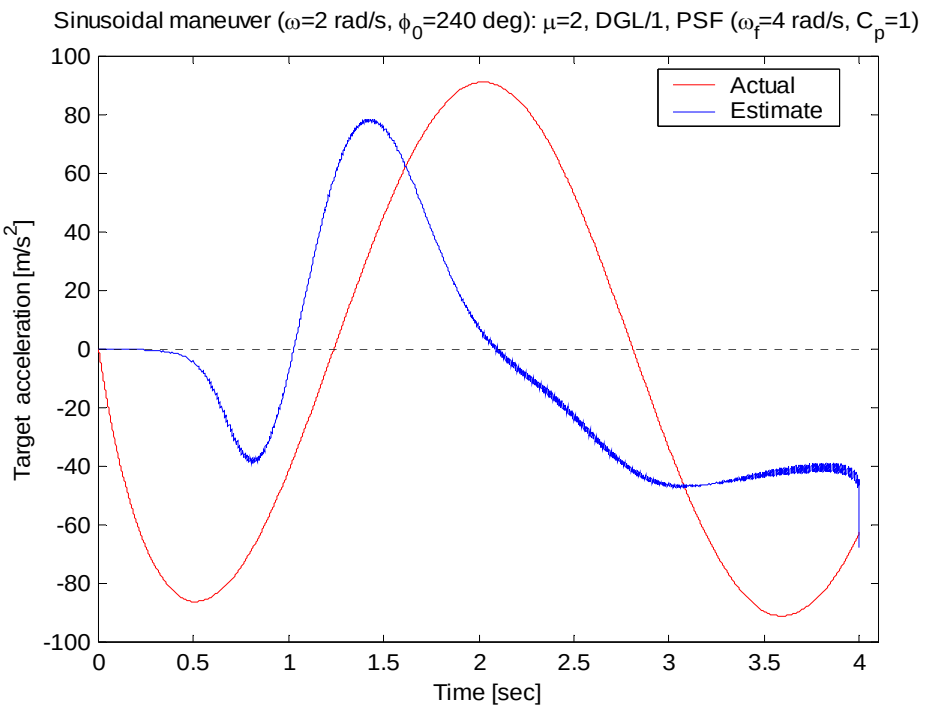

Fig. B.4. Estimation of target lateral acceleration with unmatched PSF

Table B.9a. Sinusoidal and bang-bang maneuver, DGL/1, PSF (ω_f = 2 rad/s, C_p = 1), σ_a = 0.1 mrad, r_{95} [m]

ω , rad/s / μ	0.5	1.0	1.5	2.0	2.5	3.0	bang-bang
1.5	2.49	1.78	1.08	0.55	0.51	1.07	11.5
2.0	0.85	0.69	0.43	0.3	0.29	0.48	4.23
2.5	0.50	0.44	0.32	0.21	0.21	0.37	2.50
3.0	0.40	0.35	0.25	0.15	0.16	0.30	1.78

Table B.9b. Sinusoidal and bang-bang maneuver, DGL/1, PSF (ω_f = 2 rad/s, C_p = 1), σ_a = 0.1 mrad, r_{av} [m]

ω , rad/s / μ	0.5	1.0	1.5	2.0	2.5	3.0	bang-bang
1.5	1.56	0.97	0.51	0.24	0.20	0.46	7.96
2.0	0.46	0.32	0.20	0.13	0.13	0.20	3.13
2.5	0.25	0.19	0.14	0.10	0.11	0.15	1.74
3.0	0.18	0.14	0.12	0.09	0.10	0.14	1.40

Table B.10a. Sinusoidal and bang-bang maneuver, DGL/1, PSF (ω_f = 3 rad/s, C_p = 1), σ_a = 0.1 mrad, r_{95} [m]

ω , rad/s / μ	1.5	2.0	2.5	3.0	3.5	4.0	bang-bang
1.5	3.12	1.64	0.80	0.52	0.82	2.25	15.18
2.0	1.27	0.81	0.43	0.29	0.38	0.78	3.78
2.5	0.79	0.52	0.34	0.19	0.29	0.52	1.98
3.0	0.57	0.42	0.26	0.14	0.22	0.43	1.16

Table B.10b. Sinusoidal and bang-bang maneuver, DGL/1, PSF (ω_f = 3 rad/s, C_p = 1), σ_a = 0.1 mrad, r_{av} [m]

ω , rad/s / μ	1.5	2.0	2.5	3.0	3.5	4.0	bang-bang
1.5	2.14	0.98	0.40	0.20	0.33	1.09	10.89
2.0	0.80	0.42	0.19	0.11	0.16	0.38	2.68
2.5	0.45	0.26	0.14	0.09	0.13	0.25	1.28
3.0	0.31	0.19	0.12	0.08	0.11	0.20	0.78

These numerical results are plotted in Fig. AR1.7 together with those of Tables B.6b and B.8 are plotted in Fig. B.5.

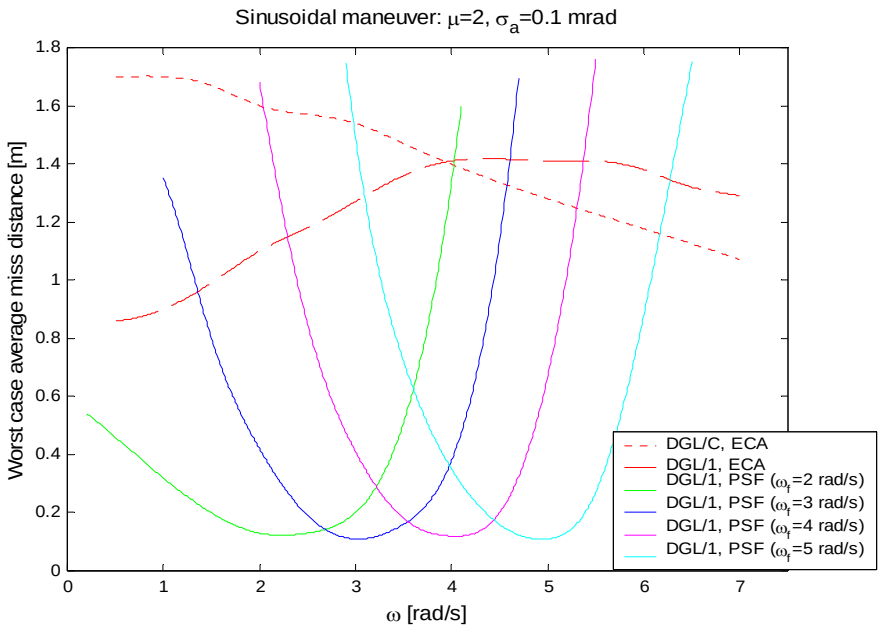

Fig. B.5. Homing performance with different estimators

From these results, one can conclude that if the mismatch between the PSF and the actual frequency is not too large (less than ± 1.0 rd/sec), the performance deterioration is acceptable. If the uncertainty of the maneuvering frequency is too large, an estimator with ECA/SF will limit the performance deterioration.

Although online estimation of the maneuver frequency might has been considered, earlier results [19] indicated that good results could be expected only if the level of the measurement noise level is very low (order of $\sigma_a = 0.01$ rd/sec), which is not a realistic assumption.

The sensitivity of the PSF estimator to frequency mismatch depends on the value of the tuning parameter C_p, as it is illustrated in Fig. B.6. A smaller value of this parameter, representing higher process noise, leads to some increase of miss distance at the "matched" frequency, but reduces the mismatch sensitivity.

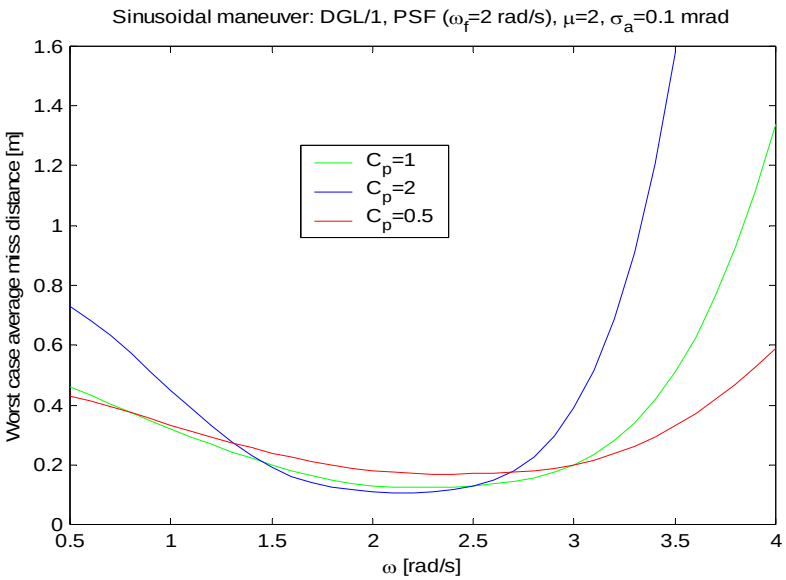

Fig. B.6. The effect of C_p on homing performance due to frequency mismatch

In Fig. B.7 the ensemble average of the estimation error in target acceleration obtained from 100 Monte Carlo runs is depicted for three estimators with different shaping filters. The ensemble average time histories clearly illustrate the origin of performance deterioration due to the use of an "unmatched" estimator. With the matched shaping filter the estimation error converges to very small values in the last part of the end game, while in the other cases (ECA or mismatched PSF) there is no convergence. The resulting average miss distances are the clear consequences of the estimation errors.

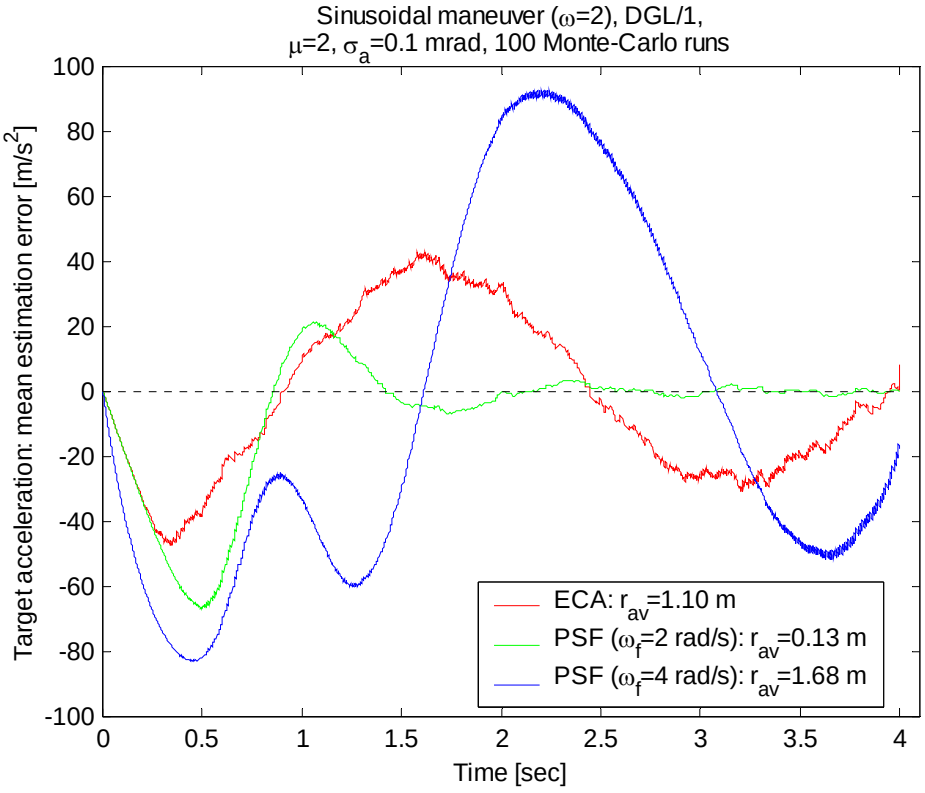

Fig. B.7. Mean estimation error of different estimators in target acceleration

Similarly, using some PSF estimator against a “bang-bang” target maneuver also reduces the homing performance, as it can be seen in Fig. B.8. Nevertheless, the performance deterioration seems less severe in these cases.

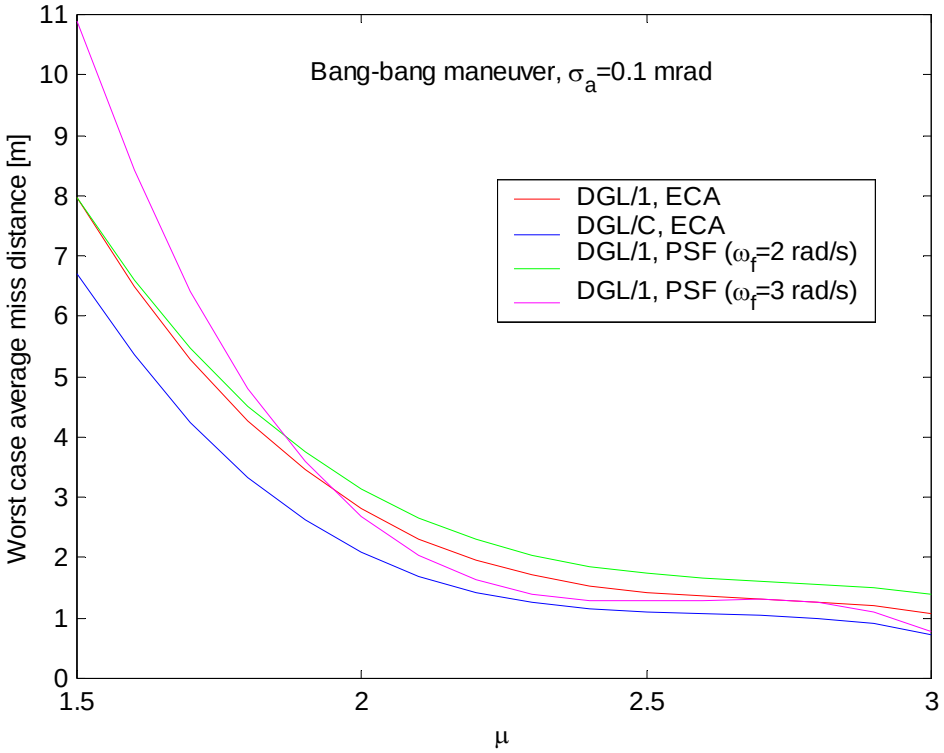

Fig. B.8. Homing performance against bang-bang maneuver

Appendix C. Estimator Equations

C.1. Estimation/guidance simulation

The numerical integration of the nonlinear equations of motion is conducted with a variable integration step Δt_i, for $0 \le t \le t_f$. The angle between the current and initial line of sight is measured with constant frequency f (100 Hz in this simulation) which gives the constant sampling period $T=f^{-1}$. The measurements are made at the moments $\hat{t}_k = kT,\ k=1,\ldots, f\, t_f$.

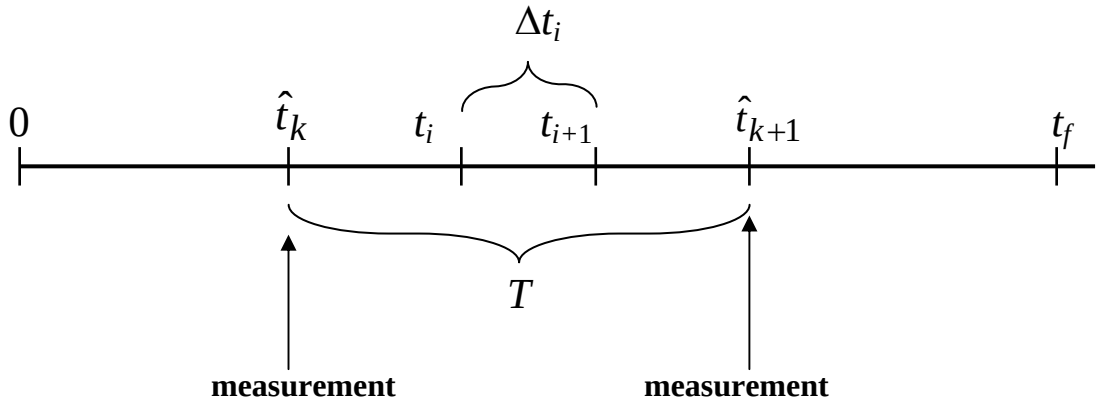

Fig. C.1. Scheme of the estimation/guidance procedure

For the sake of simplicity it is assumed that $\hat{t}_k = t_{i_k}$.

The guidance law is driven at the moment t_i by the estimates $\hat{y}_i, \hat{v}_i, \hat{a}_{ei}$ of the relative separation $y(t_i)$ between the missiles, the relative velocity $v(t_i)$ and the target acceleration $a_e(t_i)$ normal to the initial line of sight. These estimates are the outputs of a Kalman filter working in accordance with the augmented target model (shaping filter).

C.2. Target models (shaping filters)

C.2.1. ECA model (untuned)

The state vector of the target model is

$$X = [y, v, a_e, a_e^c]^T, \tag{C.1}$$

where a_e^c is the target acceleration command.

The target model is described by the differential equation

$$\dot{X} = AX + Ba_p + Cw, \tag{C.2}$$

where

$$A = \begin{bmatrix} 0 & 1 & 0 & 0 \\ 0 & 0 & 1 & 0 \\ 0 & 0 & -1/\tau_s & 1/\tau_s \\ 0 & 0 & 0 & 0 \end{bmatrix}, \tag{C.3}$$

$$B = [0,-1,0,0]^T, \tag{C.4}$$

$$C = [0,0,0,1]^T, \tag{C.5}$$

a_p is the interceptor acceleration normal to the initial line of sight;

$$w \sim W\,N(0,q), \tag{C.6}$$

$$q = \left(\frac{a_e^{\max}}{C_s} \right)^2,$$

w is the process noise, which is assumed to be zero-mean, white and Gaussian.

The tuning parameters of the ECA estimator are:

1) The decorrelation time of the maneuver τ_s,

2) The coefficient C_s of the process noise covariance q.

C.2.2. ECA model (tuned for target maneuver switch)

This model is described by the same equations (C.1) – (C.6). Additionally it is assumed that

$$a_e^c = \begin{cases} a_e^{\max}, & 0 \le t \le \tilde{t}_{sw}, \\ -a_e^{\max}, & \tilde{t}_{sw} < t < t_f, \end{cases} \tag{C.7}$$

where $\tilde{t}_{sw}$ is the switching time to which the model is tuned.

C.2.3. Periodical target model

In this case the state model vector is

$$X = [y, v, a_e, j_e]^T, \tag{C.8}$$

where j_e is the time derivative of the target acceleration (jerk). The target model is described by the differential equation (C.2) where

$$A = \begin{bmatrix} 0 & 1 & 0 & 0 \\ 0 & 0 & 1 & 0 \\ 0 & 0 & 0 & 1 \\ 0 & 0 & -\omega_f^2 & 0 \end{bmatrix}, \tag{C.9}$$

B, C and w are given by (C.4), (C.5) and (C.6), respectively.

The tuning parameters of the periodical estimator are:

1) The target frequency ω_f to which the model is tuned;

2) The coefficient C_s of the process noise covariance q.

C.3. Discrete time version

Discretization of (C.2) with time step Δt_i gives

$$X_{i+1} = F_i X_i + \Gamma_i a_{pi} + G_i w_i , \tag{C.10}$$

where

$$F_i = \exp(A\Delta t_i) , \tag{C.11}$$

$$\Gamma_i = F_i B \Delta t_i , \tag{C.12}$$

$$w_i \sim N(0, q_i), \qquad q_i = \Delta t_i \; q , \tag{C.13}$$

$$G_i = C . \tag{C.14}$$

C.4. Measurement model

The discrete-time measurements of the angle ϕ_{LOS} between the current and initial lines of sight are acquired with a zero-mean Gaussian angular measurement noise of a constant variance:

$$z_k = \phi_{LOS} + \zeta = H_k W_k + \zeta , \tag{C.15}$$

where

$$H_k = [1/r_k, 0, 0, 0]^T , \tag{C.16}$$

r_k is the range between the missiles at $t=t_k$ which is assumed to be measured accurately;

$$\zeta \sim N(0, \sigma^2_{ang}) \tag{C.17}$$

is the measurement error.

C.5. Kalman filter equations

Discrete-time Kalman filters are implemented based on the discrete-time state model (C.10) and the measurements model (C.15). The initial state estimate is

$$\hat{X}_{0/0} = (0,0,0,0)^T \ . \tag{C.18}$$

The initial covariance matrix is chosen arbitrarily as

$$P_{0/0} = \begin{bmatrix} 100 & 0 & 0 & 0 \\ 0 & 1000 & 0 & 0 \\ 0 & 0 & 1000 & 0 \\ 0 & 0 & 0 & 100 \end{bmatrix} . \tag{C.19}$$

The time propagation equations (between the measurements) are as follows.

State prediction:

$$\hat{X}_{i+1} = F_i \hat{X}_i + \Gamma_i a_{pi} \quad , i = i_k, ..., i_{k+1} - 1, \tag{C..20}$$

$$\hat{X}_{k+1/k} = \hat{X}_{i_{k+1}} \tag{C.21}$$

Measurement prediction:

$$\hat{z}_{i+1} = H_k \hat{X}_i, \qquad i = i_k, ..., i_{k+1} - 1 \ , \tag{C.22}$$

$$\hat{z}_{k+1/k} = \hat{z}_{i_{k+1}} \tag{C.23}$$

State prediction covariance:

$$P_{i+1} = F_i P_i F_i^T \ + \ q_i G_i G_i^T, \quad i = i_k, ..., i_{k+1} - 1 \ , \tag{C.24}$$

$$P_{k+1/k} = P_{i_{k+1}} \tag{C.25}$$

The measurement update equations are as follows.

Innovations process covariance:

$$S_{k+1} = H_{k+1} P_{k+1/k} H_{k+1}^T + \sigma_{\text{ang}}^2 \ , \tag{C.26}$$

Filter gain:

$$K_{k+1} = P_{k+1/k} H_{k+1}^T S_{k+1}^{-1} \ , \tag{C.27}$$

Updated state estimate:

$$\hat{X}_{k+1/k+1} = \hat{X}_{k+1/k} + K_{k+1}(z_{k+1} - \hat{z}_{k+1/k}) \ , \tag{C.28}$$

Updated state covariance:

$$P_{k+1/k+1} = P_{k+1/k} - K_{k+1} S_{k+1} K_{k+1}^T \ . \tag{C.29}$$

C.6. Identification by an Adaptive Multiple Model Estimator

To identify the target maneuver, a set of M filters are used in parallel, each tuned to some hypothesis about the target maneuver. In this case the notation refers to the filter number j with the bracketed index k : for example, $S_j(k)$ means the innovation covariance of the j –th filter after the k –th measurement. The a posteriori probability that the hypothesis representing by the j –th filter is true, is calculated as follows.

$$p_j(0) = \frac{1}{M}, \quad j = 1,...,M \ , \tag{C.30}$$

$$p_j(k) = \frac{1}{c} f_j(k) p_j(k-1) \ , \tag{C.31}$$

where the likelihood function corresponding to the j-th filter is given by

$$f_j(k) = \frac{1}{\sqrt{2\pi S_j(k)}} \exp\left(- \frac{\left(z(k) - \hat{z}_j(k/k-1)\right)^2}{2S_j(k)} \right), \tag{C.32}$$

$$c = \sum_{j=1}^{M} f_j(k) \ . \tag{C.33}$$

Appendix D. Three-dimensional Simulation Database

D.1. Target (TBM) simulation model (4 degrees of freedom)

Launch range: 600 km
Trajectory: minimum energy
Ballistic coefficient: $\beta = 5000$ kg/m^2;
Lift-to-drag ratio: $\Lambda = 2.6$

"Initial" conditions for reentry at altitude of 150 km

Velocity: $V_{e0} = 1720$ m/s
Flight path angle: $\gamma_{e0} = -18.2^o$
Horizontal distance from target: $x_{e0} = 210.3$ km

Spiral maneuver parameters

Roll damping parameter : $b = 0.004$ m^2/kg
Roll disturbance parameter: c - varying $1.8 \cdot 10^{-6} \div 4.5 \cdot 10^{-6}$ m/kg

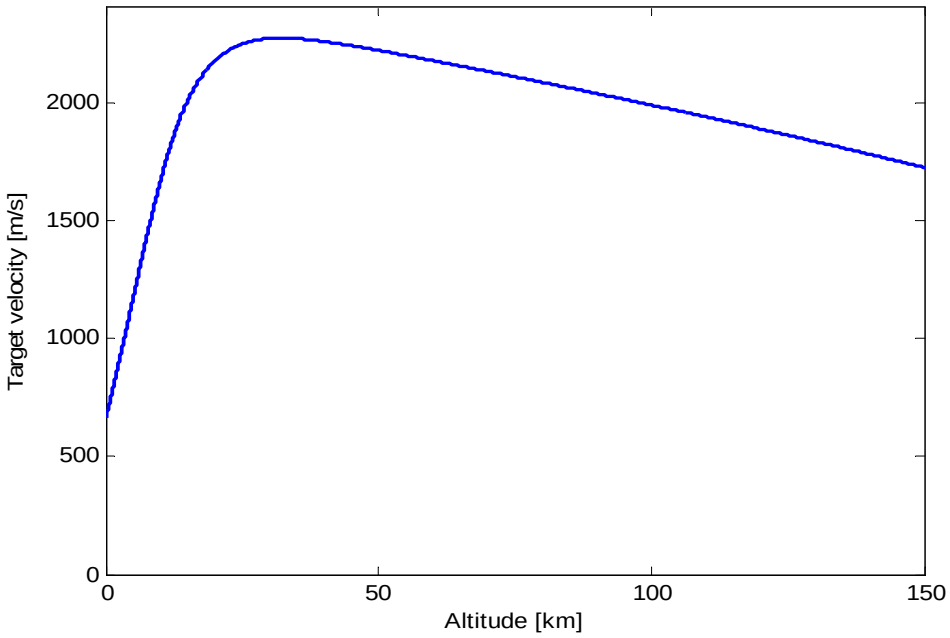

Fig. D.1. Nominal target reentry velocity profile

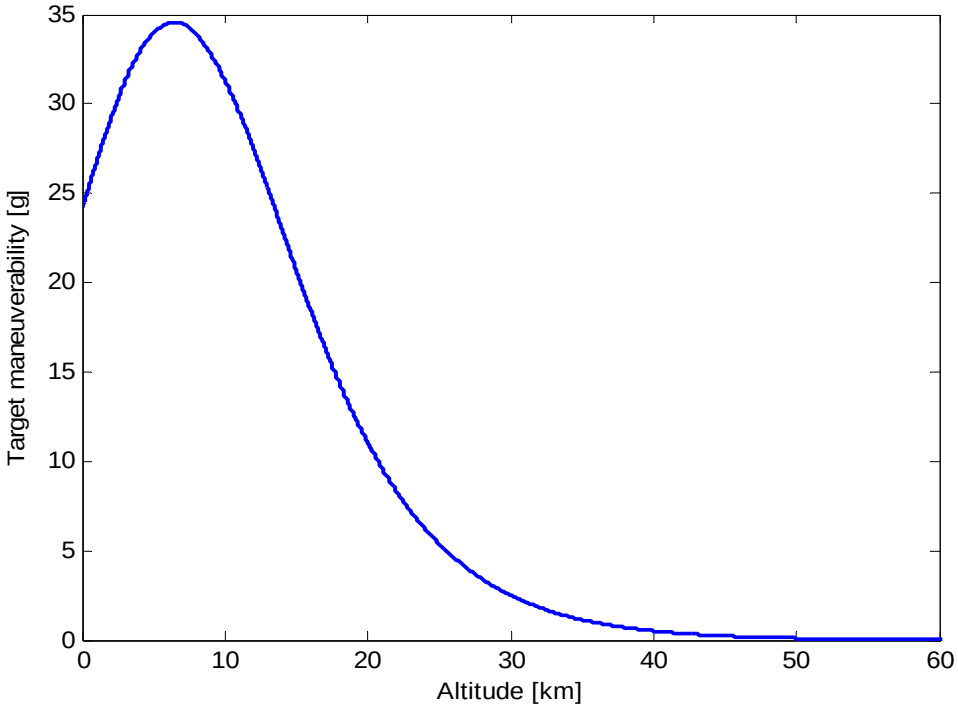

Fig. D.2. Nominal target maneuverability profile

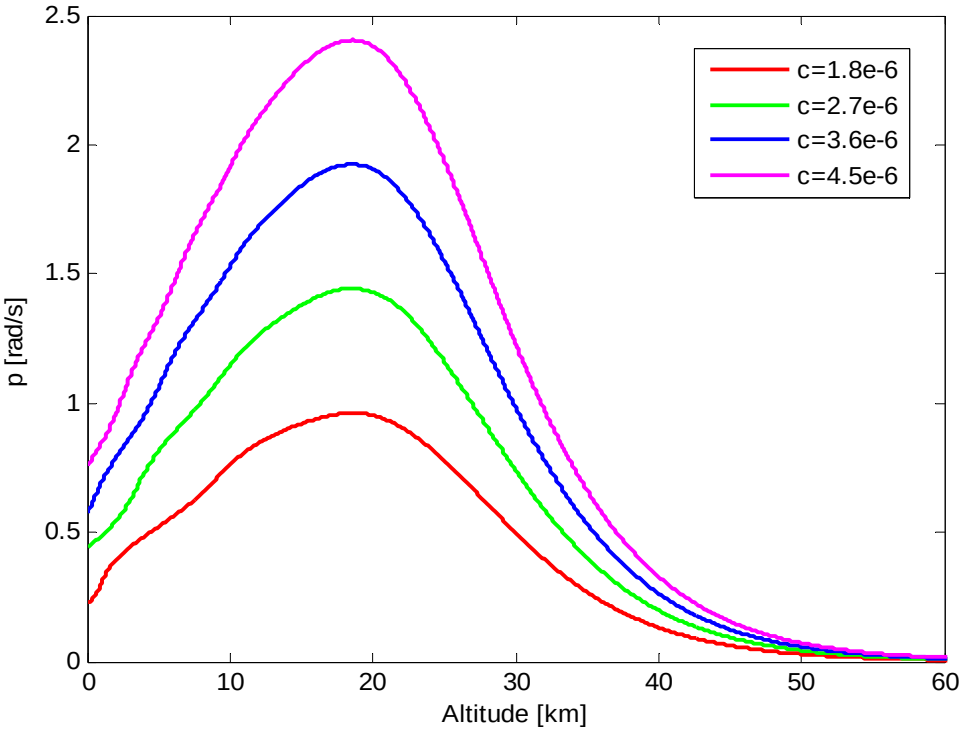

Fig. D.3. Nominal target roll rate profiles

D.2. Interceptor model

Rocket motor and aerodynamic data:

Specific impulse: I_{sp} = 250 sec.;

	t_b [sec]	T [kN]	m_0 [kg]	SC_D [m^2]	SC_{Lmax} [m^2]
1st stage	6.5	229	1540	0.10	0.24
2nd stage	13	103	781	0.05	0.20

Delay between stages:

h_{int} [km]	Δt_b [sec]
20	3
25	12
30	29

Precalculation results:

h_{int} [km]	Firing angle [deg]	Time before interception [sec]
20	63.9	21.92
25	66.1	31.47
30	70.2	48.4

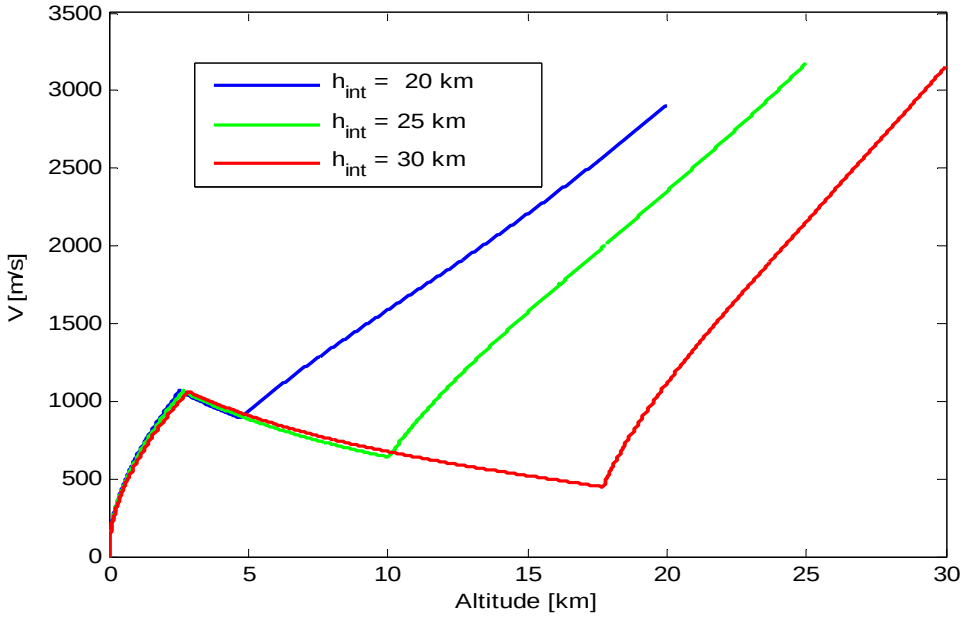

Fig. D.4. Nominal interceptor velocity profiles

D.3. Endgame initial conditions

m^*_{p0}: initial interceptor mass;
t^*_{p0}: time from interceptor launch
V^*_{i0}: initial velocity;
γ^*_{i0}: initial flight path angle;
x^*_{i0}: initial range from the interceptor launch site;
h^*_{i0}: initial altitude,

(i=p,e)

h_{int} [km]	Interceptor (pursuer)						TBM (evader)			
	m^*_{p0} [kg]	t^*_{p0} [sec]	V^*_{p0} [m/s]	γ^*_{p0} [deg]	x^*_{p0} [km]	h^*_{p0} [km]	V^*_{e0} [m/s]	γ^*_{e0} [deg]	x_{e0} [km]	h_{e0} [km]
20	442.9	17.56	1911.7	45.7	11.58	12.71	2260.4	-45.2	25.61	26.93
25	411.4	27.3	1998.8	43.6	16.01	17.78	2271.4	-44.7	30.38	31.68
30	416.5	44.18	1894.5	37.7	20.38	23.69	2265.2	-44.1	35.52	36.71

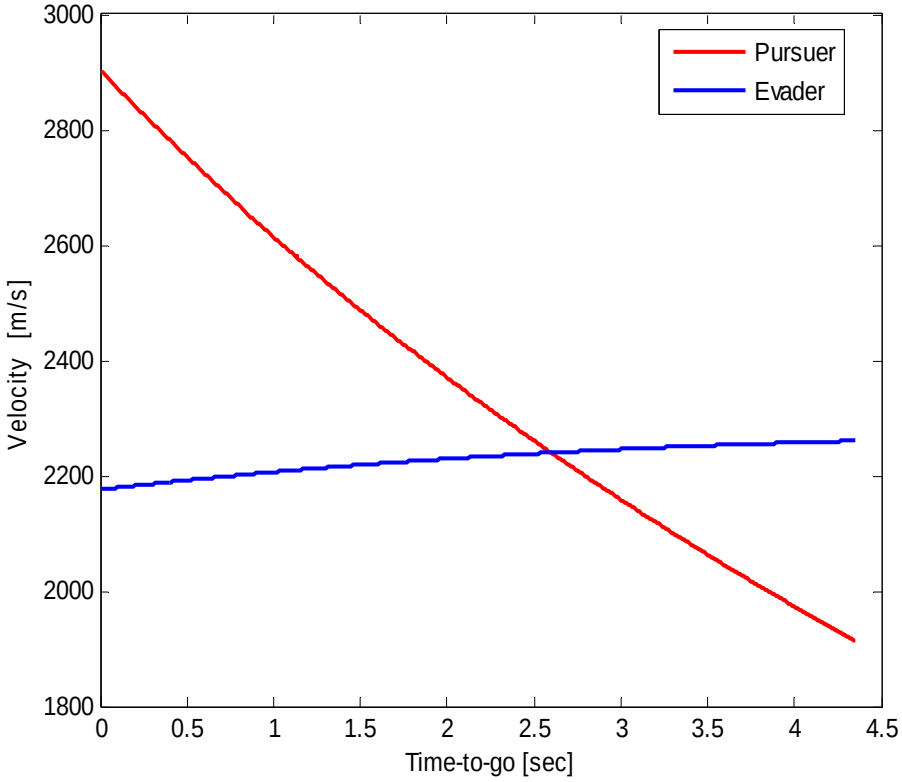

Fig. D.5. Nominal endgame velocity profiles for h_{int} = 20 km

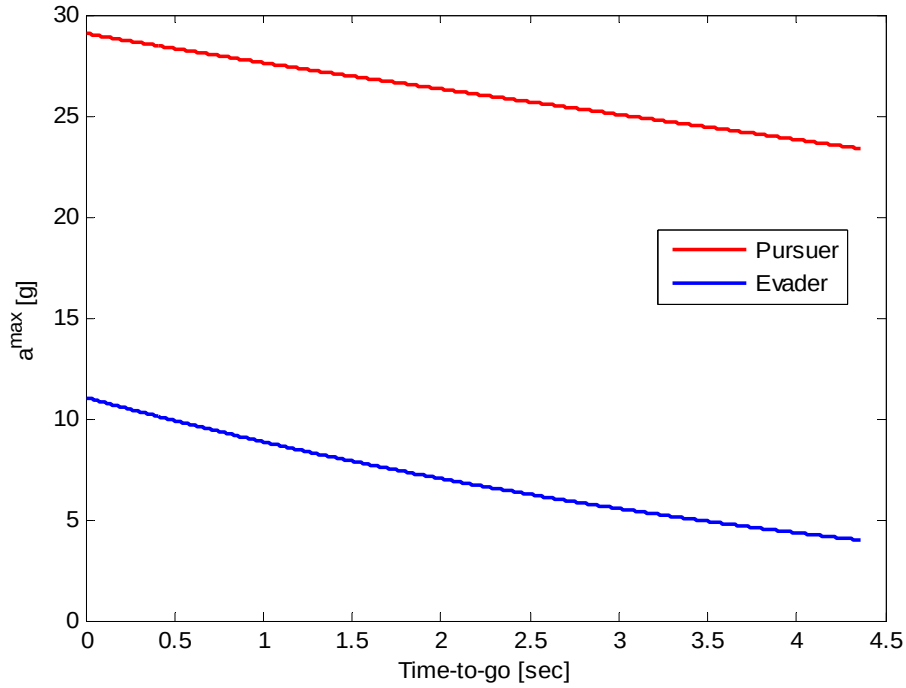

Fig. D.6. Nominal endgame maneuverability profiles for h_{int} = 20 km

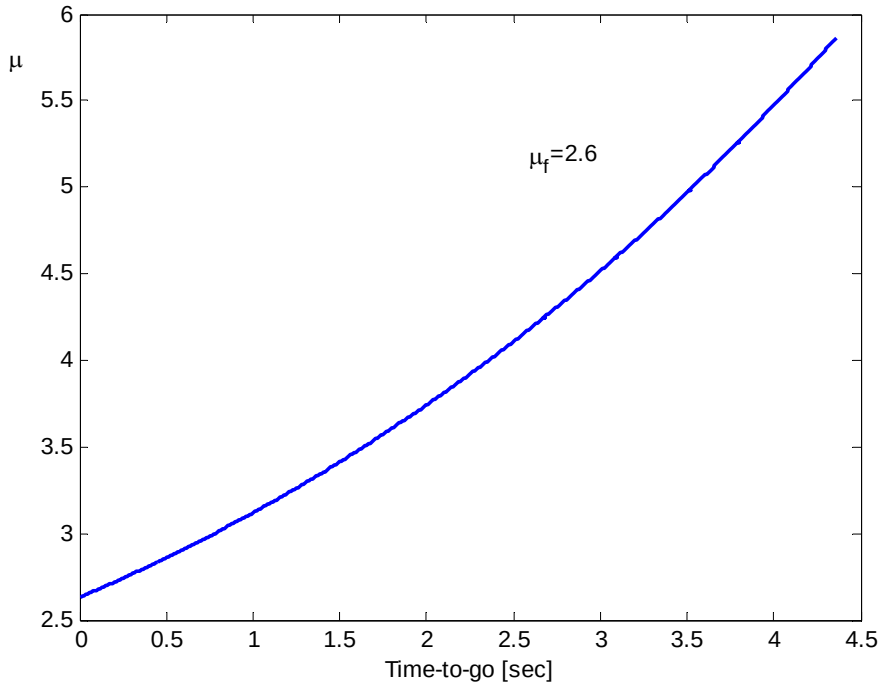

Fig. D.7. Nominal endgame maneuverability ratio for h_{int} = 20 km

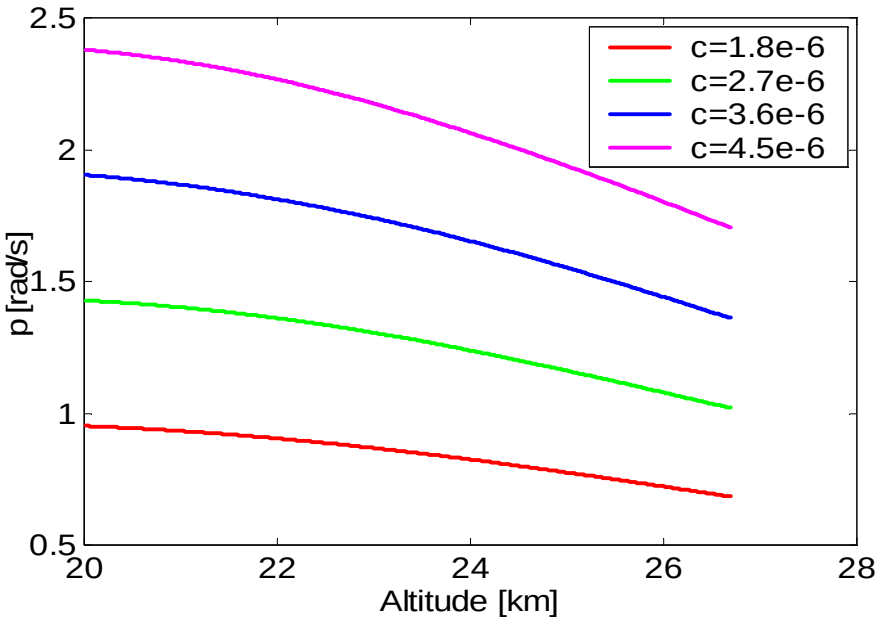

Fig. D.8. Nominal endgame roll rate profiles for h_{int} = 20 km

D.4. Endgame final conditions

t_f: endgame duration
μ_f: final maneuverability ratio

h_{int} [km]	t_f [sec]	μ_f
20	4.36	2.6
25	4.17	3.2
30	4.23	3.1